AN L^∞ SECOND ORDER CARTESIAN METHOD FOR 3D ANISOTROPIC INTERFACE PROBLEMS*

Baiying Dong

School of Mathematics and Statistics, NingXia University, Yinchuan 750021, China;
School of Mathematics and Computer Science, NingXia Normal University, Guyuan 756000, China
Email: baiying_dong@nxnu.edu.cn

Xiufeng Feng[1)]

School of Mathematics and Statistics, NingXia University, Yinchuan 750021, China
Email: xf_feng@nxu.edu.cn

Zhilin Li

Department of Mathematics, North Carolina State University, Raleigh, NC 27695-8205, USA
Email: zhilin@ncsu.edu

Abstract

A second order accurate method in the infinity norm is proposed for general three dimensional anisotropic elliptic interface problems in which the solution and its derivatives, the coefficients, and source terms all can have finite jumps across one or several arbitrary smooth interfaces. The method is based on the 2D finite element-finite difference (FE-FD) method but with substantial differences in method derivation, implementation, and convergence analysis. One of challenges is to derive 3D interface relations since there is no invariance anymore under coordinate system transforms for the partial differential equations and the jump conditions. A finite element discretization whose coefficient matrix is a symmetric semi-positive definite is used away from the interface; and the maximum preserving finite difference discretization whose coefficient matrix part is an M-matrix is constructed at irregular elements where the interface cuts through. We aim to get a sharp interface method that can have second order accuracy in the point-wise norm. We show the convergence analysis by splitting errors into several parts. Nontrivial numerical examples are presented to confirm the convergence analysis.

Mathematics subject classification: 65M06, 76M20, 65N06.
Key words: 3D anisotropic PDE, Cartesian meshes, Finite element method, Finite difference method, Maximum preserving IIM, Convergence analysis.

1. Introduction

In this paper, we develop a finite element-finite difference method for three dimensional (3D) anisotropic elliptic partial differential equations (PDEs) involving finite number of non-overlapping interfaces across which the coefficients of the PDE may be discontinuous, and the source term may be discontinuous and even can have a singular source term corresponding to a jump in the flux or the solution. The problem is described as follows,

$$-\nabla \cdot \Big(\mathbf{A}(\mathbf{x})\nabla u(\mathbf{x})\Big) + \sigma(\mathbf{x})u(\mathbf{x}) = f(\mathbf{x}), \quad \mathbf{x} = (x,y,z) \in \Omega \setminus \Gamma, \ \Omega = \Omega^+ \cup \Omega^-,$$

$$u(\mathbf{x}) = u_0(\mathbf{x}), \quad \mathbf{x} = (x,y,z) \in \partial\Omega, \tag{1.1}$$

where the coefficient matrix $\mathbf{A}(\mathbf{x}) \in C^1(\Omega \setminus \Gamma)$ is a 3×3 symmetric positive definite (SPD) matrix,

$$\mathbf{A}(\mathbf{x}) = \begin{pmatrix} A_{11}(\mathbf{x}) & A_{12}(\mathbf{x}) & A_{13}(\mathbf{x}) \\ A_{12}(\mathbf{x}) & A_{22}(\mathbf{x}) & A_{23}(\mathbf{x}) \\ A_{13}(\mathbf{x}) & A_{23}(\mathbf{x}) & A_{33}(\mathbf{x}) \end{pmatrix}, \qquad \mathbf{x} \in \Omega. \tag{1.2}$$

We define the $\mathbf{A}^+$ and $\mathbf{A}^-$ as the restrictions of $\mathbf{A}$ on Ω^+ and Ω^-, respectively,

$$\mathbf{A} = \begin{cases} \mathbf{A}^+(\mathbf{x}), & \text{if} \quad \mathbf{x} \in \Omega^+, \\ \mathbf{A}^-(\mathbf{x}), & \text{if} \quad \mathbf{x} \in \Omega^-, \end{cases} \tag{1.3}$$

where $\mathbf{A}^\pm(\mathbf{x}) \in C^1(\Omega^\pm)$. Since we use both finite element and finite difference discretization, we assume that $\sigma(\mathbf{x}) \geq 0$; $f(\mathbf{x}) \in C(\Omega \setminus \Gamma)$, and the interface Γ is C^2 within the domain Ω, see Fig. 1.1 for an illustration. We allow both of the solution and the flux to be discontinuous,

$$[u](\mathbf{X}) = w(\mathbf{X}), \quad [\mathbf{A}\nabla u \cdot \mathbf{n}](\mathbf{X}) = Q(\mathbf{X}), \quad \mathbf{X} = (X, Y, Z) \in \Gamma, \tag{1.4}$$

where $\mathbf{n}(\mathbf{X})$ is the unit normal direction at a point $\mathbf{X}$ on the interface pointing to the Ω^+ side. For the regularity requirement, we assume that $w \in C^2(\Gamma)$, and $Q \in C^1(\Gamma)$. The above two jump conditions along the boundary condition make the problem well-posed. The jumps on the interface, such as $[u](\mathbf{X})$ and $[\mathbf{A}\nabla u \cdot \mathbf{n}](\mathbf{X})$, are defined as the differences of the limiting values from different sides of the interface; for example,

$$[u](\mathbf{X}) = \lim_{\mathbf{x} \to \mathbf{X}, \mathbf{x} \in \Omega^+} u(\mathbf{x}) - \lim_{\mathbf{x} \to \mathbf{X}, \mathbf{x} \in \Omega^-} u(\mathbf{x}) = u^+ - u^-.$$
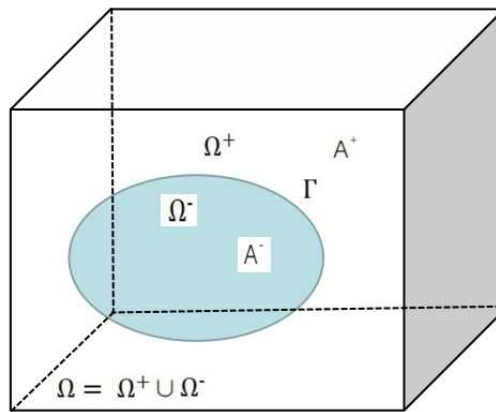

Fig. 1.1. A diagram of the anisotropic interface problem: a rectangular domain with a closed smooth interface (surface).

The existence and uniqueness of the solution is well-known based on the Lax-Milgram lemma, see for example [1]. The Galerkin finite element method can be applied to solve the problem numerically if a body-fitted 3D mesh (unstructured) can be generated, which is non-trivial and maybe time consuming. However, sometimes Cartesian methods are preferred for number of

reasons. In a Cartesian mesh method, we do not need to generate the mesh. The resulting linear system of equations can be solved by structured fast solvers; A Cartesian mesh method is often easier to be combined with other existing packages. Challenges with Cartesian methods include how to get accurate discretization near or on the interface and carry out the convergence analysis. There are limited Cartesian methods for anisotropic interface problems, mostly based on Galerkin finite element method, for example, the immersed finite element method (IFEM) in [2] or Petrov Galerkin method in [3–5], even fewer for 3D problems except for the Petrov Galerkin method in [5] and recent IFEM [6]. Note that the IFEM methods can be second order accurate in L^2 norm for 2D and 3D problems only if the discontinuous Galerkin (DG) correction terms are added along the edges of interface triangles/tetrohedrons. As far as we know, there is no proof of the convergence in the L^∞ norm for IFE or Petrov Galerkin methods. There is almost no finite difference methods for anisotropic interface problems except for the first order maximum principle preserving scheme for elliptic anisotropic PDEs on irregular domains [7], and our recent finite element-finite difference (FE-FD) method [8] for 2D elliptic anisotropic interface problems.

Our new FE-FD method proposed in this paper has some important features: it is a sharp interface method because the interface conditions are enforced and pointwise second order accuracy except by a factor $|\log h|^{4/3}$ can be proved. Our method also avoids complicated volume integrals for interface tetrahedrons. While the main ideas for 2D and 3D problems are similar, the theoretic derivation of the jump conditions, methods design and implementation are much challenging in 3D. In 2D, the interfaces are curves and there is a unique tangential direction at a point on an interface. In 3D, the interfaces are surfaces and there are two arbitrary tangent directions. There are many more terms in the interface relations in 3D compared with that in 2D.

The rest of the paper is organized as follows. In Section 2, we describe the finite element method based on a uniform tetrahedralization for regular anisotropic elliptic PDEs in 3D. In Section 3, we derive new interface relations of the 3D anisotropic elliptic interface PDEs. After those preparations, we construct the maximum principle preserving discretization at irregular grid points and present the convergence analysis. Several numerical experiments will be provided in Section 4. We conclude in the last section.

2. Finite Element Discretization for 3D Anisotropic Elliptic Problems

In this section, we use a standard finite element method to derive the discrete linear system of equations at elements away from the interface. Since a uniform mesh is used, the finite element discretization is equivalent to a finite difference discretization. We use the theory of finite element methods for the convergence proof.

We assume that the domain Ω is a cube $\Omega = [a_1, b_1] \times [a_2, b_2] \times [a_3, b_3]$. For simplicity of discussion, we use a uniform Cartesian grid

$$\begin{cases} x_i = a_1 + ih, & i = 0, 1, \cdots, L, \\ y_j = a_2 + jh, & j = 0, 1, \cdots, M, \\ z_k = a_3 + kh, & k = 0, 1, \cdots, N, \end{cases} \tag{2.1}$$

where $h = (b_1 - a_1)/l = (b_2 - a_2)/m = (b_3 - a_3)/n$. We divide every cubic cell region $[x_{i-1}, x_i] \times [y_{j-1}, y_j] \times [z_{k-1}, z_k]$ into six tetrahedral elements to have a uniform tetrahedralization

T^h, see Fig. 2.1 as an illustration. The interface Γ is represent by a zero level set of a Lipschitz
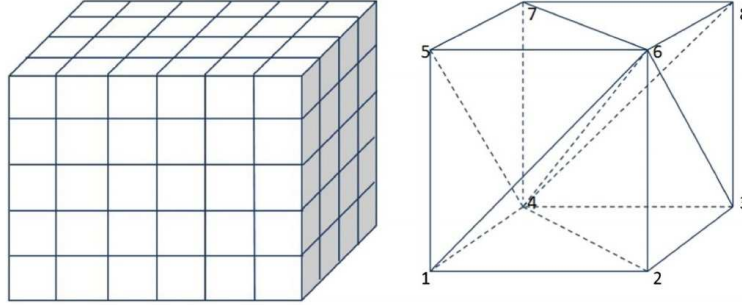

Fig. 2.1. A diagram of a cubic mesh and the uniform tetrahedralization.

continuous function $\varphi(\mathbf{x}) = \varphi(x, y, z)$, often the signed distance function,

$$\Gamma = \{(x, y, z)|\ \varphi(x, y, z) = 0,\ (x, y, z) \in \Omega\}. \tag{2.2}$$

At a grid point (x_i, y_j, z_k), we define

$$\varphi_{ijk}^{\max} = \max\{\varphi_{i-1,j,k}, \varphi_{ijk}, \varphi_{i+1,j,k}, \varphi_{i,j-1,k}, \varphi_{i,j+1,k}, \varphi_{i,j,k-1}, \varphi_{i,j,k+1},$$
$$\varphi_{i-1,j-1,k}, \varphi_{i+1,j+1,k}, \varphi_{i-1,j,k-1}, \varphi_{i+1,j,k+1}, \varphi_{i,j-1,k-1}, \varphi_{i,j+1,k+1}, \tag{2.3}$$
$$\varphi_{i-1,j-1,k-1}, \varphi_{i+1,j+1,k+1}\},$$

$$\varphi_{ijk}^{\min} = \min\{\varphi_{i-1,j,k}, \varphi_{ijk}, \varphi_{i+1,j,k}, \varphi_{i,j-1,k}, \varphi_{i,j+1,k}, \varphi_{i,j,k-1}, \varphi_{i,j,k+1},$$
$$\varphi_{i-1,j-1,k}, \varphi_{i+1,j+1,k}, \varphi_{i-1,j,k-1}, \varphi_{i+1,j,k+1}, \varphi_{i,j-1,k-1}, \varphi_{i,j+1,k+1}, \tag{2.4}$$
$$\varphi_{i-1,j-1,k-1}, \varphi_{i+1,j+1,k+1}\},$$

where $\varphi_{ijk} = \varphi(x_i, y_j, z_k)$. A grid point (x_i, y_j, z_k) is called *regular* if $\varphi_{ijk}^{\max}\varphi_{ijk}^{\min} > 0$, otherwise it is *irregular*. In this section, we discuss the finite element discretization at regular grid points.

From [9], we know that there exists a piecewise smooth function $\widehat{w} : \Omega \to \mathbb{R}$ that satisfies

$$[\widehat{w}](\mathbf{X}) = w(\mathbf{X}), \quad \mathbf{X} \in \Gamma, \qquad \widehat{w}(\mathbf{x}) = u_0(\mathbf{x}), \quad \mathbf{x} \in \partial\Omega.$$

Note that such a $\widehat{w}$ is not needed in our algorithm but useful to get the weak form. The original interface problem can be re-formulated as: find $u(\mathbf{x}) = q(\mathbf{x}) + \widehat{w}(\mathbf{x})$ with $q(\mathbf{x}) \in H_0^1(\Omega)$ such that

$$a(q, v) = \int_\Omega f v \, dx dy dz - \int_\Omega Q v \, ds - \int_\Omega \mathbf{A}\nabla\widehat{w} \cdot \nabla v \, dx dy dz, \quad v \in H_0^1(\Omega), \tag{2.5}$$

where

$$a(q, v) = \int_\Omega \left(\mathbf{A}\nabla q \cdot \nabla v + \sigma q v\right) dx dy dz$$

$$= \int_\Omega \Big(A_{11} q_x v_x + A_{22} q_y v_y + A_{33} q_z v_z + A_{12}(q_x v_y + q_y v_x)$$

$$+ A_{13}(q_x v_z + q_z v_x) + A_{23}(q_y v_z + q_z v_y) + \sigma q v\Big) dx dy dz.$$

For convenience, we also define

$$H^1(\Omega^\pm) = \{v(\mathbf{x}) \in L^2(\Omega) \mid v(\mathbf{x})|_{\mathbf{x} \in \Omega^+} \in H^1(\Omega^+); \quad v(\mathbf{x})|_{\mathbf{x} \in \Omega^-} \in H^1(\Omega^-)\}.$$

Let V_h be the standard P_1 conforming linear finite element space associated with the tetrahedral mesh. On regular nodal points at which the surrounding tetrahedrons are all on the same side of the interface, the contribution to the resulting linear system of equations is the same as the original weak form, that is, treating the last two terms in (2.5) as zero to have

$$a(u_h, v_h) = \int_\Omega f v_h dx dy dz, \qquad v_h \in V_{h,0}, \quad v_h \in H^1(\Omega^\pm), \quad v_h \cap \Gamma = \emptyset. \tag{2.6}$$

Let $\{\psi_k(x,y,z)\}_{k=1}^{N_{dof}}$ be a set of basis functions for V_h, a finite element approximation to the anisotropic problem is

$$u_h = \sum_{k=1}^{N_{dof}} \alpha_k \psi_k(x,y,z). \tag{2.7}$$

The linear system of equations are

$$\sum_{j=1}^{N_{dof}} a(\psi_i, \psi_j)\alpha_j = \int_\Omega f\psi_i dx dy dz, \quad i = 1, 2, \cdots, N_{dof}, \tag{2.8}$$

which can be written as a matrix-vector form

$$K_h \mathbf{U} = \mathbf{F}, \qquad U = (\alpha_1, \alpha_2, \cdots, \alpha_{N_{dof}})^T, \tag{2.9}$$

where the components of stiffness matrix K_h is

$$K_{ij} = \int_\Omega (\mathbf{A}\nabla\psi_i\nabla\psi_j + \sigma\psi_i\psi_j)\,dx dy dz = \sum_e \int_e (\mathbf{A}\nabla\psi_i\nabla\psi_j + \sigma\psi_i\psi_j)\,dx dy dz, \tag{2.10}$$

and the components of load vector is

$$F_i = \int_\Omega f\psi_i dx dy dz = \sum_e \int_e f\psi_i dx dy dz. \tag{2.11}$$

The discrete linear system of equations (2.9) can be regarded as a linear system of equations of a finite difference equations if the usual P_1 finite element basis functions are used since we have $\alpha_m = U_m$ that is a finite difference approximation to exact solution $u(x_i, y_j, z_k)$ at a grid point $\mathbf{x}_m = (x_i, y_j, z_k)$. If the coefficient matrix $\mathbf{A}$ is a constant matrix and σ is a constant, we can get the discrete matrix K_h exactly. For a variable coefficient matrix $\mathbf{A}(\mathbf{x})$, we use a linear interpolation from the values at the vertices to approximate $\mathbf{A}(\mathbf{x})$,

$$\mathbf{A}(\mathbf{x}) \approx \sum_k^{N_{dof}} \mathbf{A}(\mathbf{x}_k)\psi_k(\mathbf{x}), \tag{2.12}$$

with an $O(h^2)$ error. We also approximate the entries of the mass matrix at $\mathbf{x}_m = (x_i, y_j, z_k)$ by

$$\int_\Omega \sigma(\mathbf{x})\psi_m(\mathbf{x})\psi_n(\mathbf{x})d\mathbf{x} \approx \delta_{mn}\sigma(\mathbf{x}_m)h^3 = \delta_{mn}\sigma_{ijk}h^3, \tag{2.13}$$

with the contribution from a local element e as,

$$\int_e \sigma(\mathbf{x})\psi_m^e(\mathbf{x})\psi_n^e(\mathbf{x})d\mathbf{x} \approx \frac{V^e}{4}\sum_{l=1}^{4}\sigma(\mathbf{x}_l^e)\psi_m^e(\mathbf{x}_l^e)\psi_n^e(\mathbf{x}_l^e) = \frac{V^e}{4}\delta_{mn}\sigma_{ijk}, \tag{2.14}$$

where $\sigma_{ijk} = \sigma(x_i, y_j, z_k)$. Similarly, we approximate the load vector at $\mathbf{x}_m = (x_i, y_j, z_k)$ as

$$\int_\Omega f(\mathbf{x})\psi_m(\mathbf{x})d\mathbf{x} \approx f_{ijk}h^3, \tag{2.15}$$

with the contribution from a local element e as

$$\int_e f(\mathbf{x})\psi_m^e(\mathbf{x})d\mathbf{x} \approx \frac{V^e}{4}\sum_{l=1}^{4}f(\mathbf{x}_l^e)\psi_m^e(\mathbf{x}_l^e) = \frac{V^e}{4}f_{ijk}, \tag{2.16}$$

where $f_{ijk} = f(x_i, y_j, z_k)$. Note that the error in approximating the weak form ((2.13)-(2.16)) has the same order as that of the classical P_1 finite element method for second order elliptic PDES, that is, $O(h^2)$ in L^2 norm globally ($O(h^4)$ on each element), see for example, [10,11] for more details. This is in line with the piecewise linear approximation to the solution. We use the piecewise linear approximation to approximate $f(\mathbf{x})$, $\mathbf{A}(\mathbf{x})$ and $\sigma(\mathbf{x})$.

If the coefficient matrix $\mathbf{A}(x, y, z)$ is a constant matrix, by some derivations and calculations, the resulting linear equation at a node (x_i, y_j, z_k) can be written as

$$\begin{aligned}
&\frac{6A_{11} + 6A_{22} + 6A_{33} - 4A_{12} - 4A_{13} - 4A_{23}}{3h^2}U_{ijk} + \sigma U_{ijk} \\
&- \frac{A_{12} + A_{13} + A_{23}}{3h^2}\left(U_{i-1,j-1,k-1} + U_{i+1,j+1,k+1}\right) \\
&+ \frac{-3A_{11} + 2A_{12} + 2A_{13} - A_{23}}{3h^2}\left(U_{i-1,j,k} + U_{i+1,j,k}\right) \\
&+ \frac{-3A_{22} + 2A_{12} - A_{13} + 2A_{23}}{3h^2}\left(U_{i,j-1,k} + U_{i,j+1,k}\right) \\
&+ \frac{-3A_{33} - A_{12} + 2A_{13} + 2A_{23}}{3h^2}\left(U_{i,j,k-1} + U_{i,j,k+1}\right) \\
&+ \frac{-2A_{12} + A_{13} + A_{23}}{3h^2}\left(U_{i-1,j-1,k} + U_{i+1,j+1,k}\right) \\
&+ \frac{A_{12} - 2A_{13} + A_{23}}{3h^2}\left(U_{i-1,j,k-1} + U_{i+1,j,k+1}\right) \\
&+ \frac{A_{12} + A_{13} - 2A_{23}}{3h^2}\left(U_{i,j-1,k-1} + U_{i,j+1,k+1}\right) = f_{ijk}.
\end{aligned} \tag{2.17}$$

The resulted finite difference discretization has a fifteen-point stencil and the resulting coefficient matrix is a symmetric positive definite. We have shown that the local truncation errors of the finite difference discretization (2.17) at a grid point (x_i, y_j, z_k) is bounded by (so it is consistent)

$$|T_{ijk}| \leq C\max_{|\alpha|\leq 4}|D^\alpha u|h^2, \tag{2.18}$$

where $D^\alpha u$ is a multi-index of partial derivatives defined as

$$D^\alpha u(\mathbf{x}) = \frac{\partial^{|\alpha|}u(\mathbf{x})}{\partial x^{\alpha_1}\partial y^{\alpha_2}\partial z^{\alpha_3}}, \qquad |\alpha| = \alpha_1 + \alpha_2 + \alpha_3, \quad \alpha_i \geq 0, \; i = 1, 2, 3. \tag{2.19}$$

From the classical finite element method convergence analysis and Nitch's trick, see [12–14], we also know that the finite difference scheme (2.17) (also a finite element method) is second order accurate in the infinity norm for non-interface problems with the following error estimate,

$$\max_{ijk} \left| u(x_i, y_j, z_k) - U_{ijk} \right| \leq C |\log h|^{4/3} h^2, \tag{2.20}$$

where U_{ijk} is the approximate solution to $u(x_i, y_j, z_k)$ obtained by the scheme (2.17) at a grid point $\mathbf{x}_m = (x_i, y_j, z_k)$.

The estimate (2.20) was proved in [12] for three-dimensional elliptic problems. Note that for non-interface anisotropic problems with a constant matrix $\mathbf{A}$, we can apply a scaling and rotating transformation to transform the original problem to a scalar elliptic PDE. The transformation matrix is a constant matrix and invertible, thus the estimate is valid for 3D anisotropic elliptic problems with a different error constant.

3. The Maximum Principle Preserving Discretization at Irregular Grid Points

In this section, we will develop the maximum principle preserving finite difference discretization for 3D anisotropic elliptic interface problems at irregular grid points. Because of the tensor coefficients matrix and the mixed derivatives, u_{xy}, u_{xz}, and u_{yz}, involved in PDE, the interface relations derived in [15] for 3D isotropic elliptic interface problem are not valid for anisotropic interface problems. We begin with derivation of new interface relations on the interface.

3.1. Interface relations for 3D anisotropic elliptic interface problems

It is more natural sometimes to use the local coordinates in the normal and tangential directions. We establish a local coordinate system at a point (X^*, Y^*, Z^*) on the interface Γ using the normal direction ξ and two orthogonal directions tangential to Γ, η and τ. The local coordinate system is defined as follows

$$\begin{cases} \xi = (x - X^*)\alpha_{x\xi} + (y - Y^*)\alpha_{y\xi} + (z - Z^*)\alpha_{z\xi}, \\ \eta = (x - X^*)\alpha_{x\eta} + (y - Y^*)\alpha_{y\eta} + (z - Z^*)\alpha_{z\eta}, \\ \tau = (x - X^*)\alpha_{x\tau} + (y - Y^*)\alpha_{y\tau} + (z - Z^*)\alpha_{z\tau}, \end{cases} \tag{3.1}$$

where $\alpha_{x\xi}$ is the directional cosine between x-axis and ξ, others being defined similarly. The above local coordinate system can also be written in a matrix-vector form given below

$$\begin{pmatrix} \xi \\ \eta \\ \tau \end{pmatrix} = D \begin{pmatrix} x - X^* \\ y - Y^* \\ z - Z^* \end{pmatrix}, \tag{3.2}$$

where

$$D = (d_{ij})_{3\times3} = \begin{pmatrix} \alpha_{x\xi} & \alpha_{y\xi} & \alpha_{z\xi} \\ \alpha_{x\eta} & \alpha_{y\eta} & \alpha_{z\eta} \\ \alpha_{x\tau} & \alpha_{y\tau} & \alpha_{z\tau} \end{pmatrix}.$$

At a neighborhood of the point (X^*, Y^*, Z^*), the interface can be expressed as

$$\xi = \chi(\eta, \tau), \quad \text{with} \quad \chi(0, 0) = 0, \quad \chi_\eta(0, 0) = 0, \quad \chi_\tau(0, 0) = 0. \tag{3.3}$$

By some simple calculations, we can easily verify that $D^T D = D D^T = I$ and for any differentiable function $p(x, y, z)$ we have

$$\begin{pmatrix} \overline{p}_\xi \\ \overline{p}_\eta \\ \overline{p}_\tau \end{pmatrix} = D \begin{pmatrix} p_x \\ p_y \\ p_z \end{pmatrix}, \tag{3.4}$$

and

$$\begin{pmatrix} \overline{p}_{\xi\xi} & \overline{p}_{\xi\eta} & \overline{p}_{\xi\tau} \\ \overline{p}_{\eta\xi} & \overline{p}_{\eta\eta} & \overline{p}_{\eta\tau} \\ \overline{p}_{\tau\xi} & \overline{p}_{\tau\eta} & \overline{p}_{\tau\tau} \end{pmatrix} = D \begin{pmatrix} p_{xx} & p_{xy} & p_{xz} \\ p_{yx} & p_{yy} & p_{yz} \\ p_{zx} & p_{zy} & p_{zz} \end{pmatrix} D^T, \tag{3.5}$$

where D^T is the transpose of D, I is the identity matrix, and $\overline{p}(\xi, \eta, \tau) = p(x, y, z)$. For simplicity of the presentation, we still use $p(\xi, \eta, \tau)$ to represent the $\overline{p}(\xi, \eta, \tau)$ below. From (3.5), we have

$$\begin{pmatrix} u_{xx} & u_{xy} & u_{xz} \\ u_{yx} & u_{yy} & u_{yz} \\ u_{zx} & u_{zy} & u_{zz} \end{pmatrix} = D^T \begin{pmatrix} u_{\xi\xi} & u_{\xi\eta} & u_{\xi\tau} \\ u_{\eta\xi} & u_{\eta\eta} & u_{\eta\tau} \\ u_{\tau\xi} & u_{\tau\eta} & u_{\tau\tau} \end{pmatrix} D. \tag{3.6}$$

Let

$$\begin{cases} \mathbf{r_1} = (\alpha_{x\xi}, \alpha_{y\xi}, \alpha_{z\xi}), \\ \mathbf{r_2} = (\alpha_{x\eta}, \alpha_{y\eta}, \alpha_{z\eta}), \\ \mathbf{r_3} = (\alpha_{x\tau}, \alpha_{y\tau}, \alpha_{z\tau}), \end{cases}$$

and define the following new coefficients

$$a_{ij} = \mathbf{r_i} \mathbf{A} \mathbf{r_j^T}, \qquad i, j = 1, 2, 3. \tag{3.7}$$

If the coefficient matrix $\mathbf{A}$ is a piecewise constant matrix, then we can rewrite the PDE (1.1) using the local coordinates as

$$-(a_{11} u_{\xi\xi} + a_{22} u_{\eta\eta} + a_{33} u_{\tau\tau} + 2a_{12} u_{\xi\eta} + 2a_{13} u_{\xi\tau} + 2a_{23} u_{\eta\tau}) + \sigma u = f. \tag{3.8}$$

Under the local coordinate system, we have the following theorem of interface relations for the anisotropic interface problem.

Theorem 3.1. *If $u(x, y, z) \in C^2(\Omega^\pm)$, $f(x, y, z) \in C(\Omega^\pm)$, $\Gamma \in C^2$, $w \in C^2$, $Q \in C^1$, the coefficients $\mathbf{A}$ is a piecewise constant matrix, and σ is a piecewise constant, then we have the following ten interface relations under the local coordinate system:*

$$u^+ = u^- + w, \quad u^+_\eta = u^-_\eta + w_\eta, \quad u^+_\tau = u^-_\tau + w_\tau,$$

$$u^+_\xi = \frac{a^-_{11}}{a^+_{11}}u^-_\xi - \frac{[a_{12}]}{a^+_{11}}u^-_\eta - \frac{[a_{13}]}{a^+_{11}}u^-_\tau - \frac{a^+_{12}}{a^+_{11}}w_\eta - \frac{a^+_{13}}{a^+_{11}}w_\tau + \frac{Q}{a^+_{11}},$$

$$u^+_{\eta\eta} = \chi_{\eta\eta}\frac{[a_{11}]}{a^+_{11}}u^-_\xi + \chi_{\eta\eta}\frac{[a_{12}]}{a^+_{11}}u^-_\eta + \chi_{\eta\eta}\frac{[a_{13}]}{a^+_{11}}u^-_\tau + u^-_{\eta\eta} + \chi_{\eta\eta}\frac{a^+_{12}}{a^+_{11}}w_\eta + \chi_{\eta\eta}\frac{a^+_{13}}{a^+_{11}}w_\tau - \chi_{\eta\eta}\frac{Q}{a^+_{11}} + w_{\eta\eta},$$

$$u^+_{\tau\tau} = \chi_{\tau\tau}\frac{[a_{11}]}{a^+_{11}}u^-_\xi + \chi_{\tau\tau}\frac{[a_{12}]}{a^+_{11}}u^-_\eta + \chi_{\tau\tau}\frac{[a_{13}]}{a^+_{11}}u^-_\tau + u^-_{\tau\tau} + \chi_{\tau\tau}\frac{a^+_{12}}{a^+_{11}}w_\eta + \chi_{\tau\tau}\frac{a^+_{13}}{a^+_{11}}w_\tau - \chi_{\tau\tau}\frac{Q}{a^+_{11}} + w_{\tau\tau},$$

$$u^+_{\eta\tau} = \chi_{\eta\tau}\frac{[a_{11}]}{a^+_{11}}u^-_\xi + \chi_{\eta\tau}\frac{[a_{12}]}{a^+_{11}}u^-_\eta + \chi_{\eta\tau}\frac{[a_{13}]}{a^+_{11}}u^-_\tau + u^-_{\eta\tau} + \chi_{\eta\tau}\frac{a^+_{12}}{a^+_{11}}w_\eta + \chi_{\eta\tau}\frac{a^+_{13}}{a^+_{11}}w_\tau - \chi_{\eta\tau}\frac{Q}{a^+_{11}} + w_{\eta\tau},$$

$$u^+_{\xi\eta} = S_{m1}u^-_\xi + S_{m3}u^-_\eta + S_{m5}u^-_\tau + \frac{a^-_{11}}{a^+_{11}}u^-_{\xi\eta} - \frac{[a_{12}]}{a^+_{11}}u^-_{\eta\eta} - \frac{[a_{13}]}{a^+_{11}}u^-_{\eta\tau} + S_{n1}w_\xi + S_{n3}w_\eta + S_{n5}Q$$

$$-\frac{a^+_{12}}{a^+_{11}}w_{\eta\eta} - \frac{a^+_{13}}{a^+_{11}}w_{\eta\tau} + \frac{Q_\eta}{a^+_{11}},$$

$$u^+_{\xi\tau} = S_{m2}u^-_\xi + S_{m4}u^-_\eta + S_{m6}u^-_\tau + \frac{a^-_{11}}{a^+_{11}}u^-_{\xi\tau} - \frac{[a_{12}]}{a^+_{11}}u^-_{\eta\tau} - \frac{[a_{13}]}{a^+_{11}}u^-_{\tau\tau} + S_{n2}w_\xi + S_{n4}w_\eta + S_{n6}Q$$

$$-\frac{a^+_{12}}{a^+_{11}}w_{\eta\tau} - \frac{a^+_{13}}{a^+_{11}}w_{\tau\tau} + \frac{Q_\tau}{a^+_{11}},$$

$$u^+_{\xi\xi} = C_{1,1}u^-_\xi + C_{1,2}u^-_\eta + C_{1,3}u^-_\tau + \frac{a^-_{11}}{a^+_{11}}u^-_{\xi\xi} + \frac{2a^+_{12}[a_{12}] - a^+_{11}[a_{22}]}{(a^+_{11})^2}u^-_{\eta\eta} + \frac{2a^+_{13}[a_{13}] - a^+_{11}[a_{33}]}{(a^+_{11})^2}u^-_{\tau\tau}$$

$$+\frac{2\left(a^+_{11}a^-_{12} - a^-_{11}a^+_{12}\right)}{(a^+_{11})^2}u^-_{\xi\eta} + \frac{2\left(a^+_{11}a^-_{13} - a^-_{11}a^+_{13}\right)}{(a^+_{11})^2}u^-_{\xi\tau} + \frac{2\left(a^+_{12}[a_{13}] + a^+_{13}[a_{12}] - a^+_{11}[a_{23}]\right)}{(a^+_{11})^2}u^-_{\eta\tau}$$

$$+C_{1,4}w_\eta + C_{1,5}w_\tau + \frac{2(a^+_{12})^2 - a^+_{11}a^+_{22}}{(a^+_{11})^2}w_{\eta\eta} + \frac{2(a^+_{13})^2 - a^+_{11}a^+_{33}}{(a^+_{11})^2}w_{\tau\tau} + \frac{2(a^+_{12}a^+_{13} - a^+_{11}a^+_{23})}{(a^+_{11})^2}w_{\eta\tau}$$

$$+C_{1,6}Q - \frac{2a^+_{12}}{(a^+_{11})^2}Q_\eta - \frac{2a^+_{13}}{(a^+_{11})^2}Q_\tau + \frac{\sigma^+}{a^+_{11}}w + \frac{[\sigma]}{a^+_{11}}u^- - \frac{[f]}{a^+_{11}},$$

where the unspecified coefficients can be found in the Appendix.

Proof. We obtain the first interface relation directly from $[u] = w$. Differentiating $[u] = w$ with respect to η and τ, respectively, we get

$$[u_\xi]\chi_\eta + [u_\eta] = w_\eta, \tag{3.9}$$

$$[u_\xi]\chi_\tau + [u_\tau] = w_\tau. \tag{3.10}$$

Using $\chi_\eta(0,0) = \chi_\tau(0,0) = 0$, we have the second and third relations. Differentiating (3.9) with respect to η and τ, respectively, yields

$$\chi_\eta\frac{\partial}{\partial\eta}[u_\xi] + \chi_{\eta\eta}[u_\xi] + \chi_\eta[u_{\eta\xi}] + [u_{\eta\eta}] = w_{\eta\eta}, \tag{3.11}$$

$$\chi_\eta\frac{\partial}{\partial\tau}[u_\xi] + \chi_{\eta\tau}[u_\xi] + \chi_\tau[u_{\eta\xi}] + [u_{\eta\tau}] = w_{\eta\tau}. \tag{3.12}$$

From these two jump conditions, we get the fifth and seventh interface relations. Differentiating (3.10) with respect to τ, we obtain the sixth identity below

$$\chi_\tau\frac{\partial}{\partial\tau}[u_\xi] + \chi_{\tau\tau}[u_\xi] + \chi_\tau[u_{\tau\xi}] + [u_{\tau\tau}] = w_{\tau\tau}. \tag{3.13}$$

Let $\varphi(x,y,y) = 0$ be a level set representation of the interface Γ, then the normal direction at a point $(X^*, Y^*, Z^*) \in \Gamma$ is

$$\mathbf{n} = \left. \frac{\nabla \varphi}{|\nabla \varphi|} \right|_{(X^*, Y^*, Z^*)}. \tag{3.14}$$

According to (3.4), we have

$$\begin{cases} \nabla \varphi = (\varphi_x, \varphi_y, \varphi_z)^T = D^T (\varphi_\xi, \varphi_\eta, \varphi_\tau)^T, \\ (\nabla \varphi)^T \nabla \varphi = (\varphi_\xi, \varphi_\eta, \varphi_\tau) D D^T (\varphi_\xi, \varphi_\eta, \varphi_\tau)^T = \varphi_\xi^2 + \varphi_\eta^2 + \varphi_\tau^2, \\ \mathbf{n} = \dfrac{D^T (\varphi_\xi, \varphi_\eta, \varphi_\tau)^T}{\sqrt{\varphi_\xi^2 + \varphi_\eta^2 + \varphi_\tau^2}}. \end{cases} \tag{3.15}$$

Using the equation (3.3) of the interface on the local coordinate system, we have

$$\frac{(\varphi_\xi, \varphi_\eta, \varphi_\tau)^T}{\sqrt{\varphi_\xi^2 + \varphi_\eta^2 + \varphi_\tau^2}} = \frac{(1, -\chi_\eta, \chi_\tau)^T}{\sqrt{1 + \chi_\eta^2 + \chi_\tau^2}}, \qquad \mathbf{n} = \frac{D^T (1, -\chi_\eta, -\chi_\tau)^T}{\sqrt{1 + \chi_\eta^2 + \chi_\tau^2}}. \tag{3.16}$$

Hence, we derive that

$$\begin{aligned} \mathbf{A} \nabla u \cdot \mathbf{n} = \mathbf{n}^T \mathbf{A} \nabla u &= \frac{1}{\sqrt{1 + \chi_\eta^2 + \chi_\tau^2}} (1, -\chi_\eta, -\chi_\tau) \, D \mathbf{A} D^T (u_\xi, u_\eta, u_\tau)^T \\ &= \frac{1}{\sqrt{1 + \chi_\eta^2 + \chi_\tau^2}} (1, -\chi_\eta, -\chi_\tau)(\mathbf{r_1}, \mathbf{r_2}, \mathbf{r_3})^T \mathbf{A}(\mathbf{r_1^T}, \mathbf{r_2^T}, \mathbf{r_3^T})(u_\xi, u_\eta, u_\tau)^T \\ &= \frac{1}{\sqrt{1 + \chi_\eta^2 + \chi_\tau^2}} (1, -\chi_\eta, -\chi_\tau) \begin{pmatrix} \mathbf{r_1 A r_1^T} & \mathbf{r_1 A r_2^T} & \mathbf{r_1 A r_3^T} \\ \mathbf{r_2 A r_1^T} & \mathbf{r_2 A r_2^T} & \mathbf{r_2 A r_3^T} \\ \mathbf{r_3 A r_1^T} & \mathbf{r_3 A r_2^T} & \mathbf{r_3 A r_3^T} \end{pmatrix} \begin{pmatrix} u_\xi \\ u_\eta \\ u_\tau \end{pmatrix} \\ &= \frac{1}{\sqrt{1 + \chi_\eta^2 + \chi_\tau^2}} (1, -\chi_\eta, -\chi_\tau) \begin{pmatrix} a_{11} & a_{12} & a_{13} \\ a_{12} & a_{22} & a_{23} \\ a_{13} & a_{23} & a_{33} \end{pmatrix} \begin{pmatrix} u_\xi \\ u_\eta \\ u_\tau \end{pmatrix} \\ &= \frac{1}{\sqrt{1 + \chi_\eta^2 + \chi_\tau^2}} \Big\{ (a_{11} - \chi_\eta a_{12} - \chi_\tau a_{13}) u_\xi + (a_{12} - \chi_\eta a_{22} - \chi_\tau a_{23}) u_\eta \\ &\quad + (a_{13} - \chi_\eta a_{23} - \chi_\tau a_{33}) u_\tau \Big\}. \end{aligned} \tag{3.17}$$

From this formula, the flux jump condition $[\mathbf{A} \nabla u \cdot \mathbf{n}] = Q$ can be written as

$$\begin{aligned} &[(a_{11} - \chi_\eta a_{12} - \chi_\tau a_{13}) u_\xi] + [(a_{12} - \chi_\eta a_{22} - \chi_\tau a_{23}) u_\eta] \\ &\quad + [(a_{13} - \chi_\eta a_{23} - \chi_\tau a_{33}) u_\tau] = \sqrt{1 + \chi_\eta^2 + \chi_\tau^2} \, Q, \end{aligned} \tag{3.18}$$

which leads to the fourth interface relation. Differentiating the flux jump condition (3.18) with respect to η and τ, respectively leads to

$$\begin{aligned} &[a_{11} u_{\xi\eta}] + [a_{12} u_{\eta\eta}] + [a_{13} u_{\eta\tau}] \\ &\quad - [\chi_{\eta\eta} a_{12} + \chi_{\eta\tau} a_{13}) u_\xi] - [\chi_{\eta\eta} a_{22} + \chi_{\eta\tau} a_{23}) u_\eta] - [\chi_{\eta\eta} a_{23} + \chi_{\eta\tau} a_{33}) u_\tau] = Q_\eta, \end{aligned} \tag{3.19}$$

and

$$
\begin{aligned}
&[a_{11}u_{\xi\tau}] + [a_{12}u_{\eta\tau}] + [a_{13}u_{\tau\tau}] \\
&- [\chi_{\eta\tau}a_{12} + \chi_{\tau\tau}a_{13})u_\xi] - [\chi_{\eta\tau}a_{22} + \chi_{\tau\tau}a_{23})u_\eta] - [\chi_{\eta\tau}a_{23} + \chi_{\tau\tau}a_{33})u_\tau] = Q_\tau.
\end{aligned}
\tag{3.20}
$$

The eighth and ninth interface relations are results from these two equations. The last interface relation is derived from the PDE using

$$
-([a_{11}u_{\xi\xi}] + [a_{22}u_{\eta\eta}] + [a_{33}u_{\tau\tau}] + 2[a_{12}u_{\xi\eta}] + 2[a_{13}u_{\xi\tau}] + 2[a_{23}u_{\eta\tau}]) + [\sigma u] = [f], \tag{3.21}
$$

and using the already derived interface conditions and some tedious manipulations. □

Remark 3.1. If the coefficient matrix $\mathbf{A}(\mathbf{x})$ and $\sigma(\mathbf{x})$ are piecewise variable functions, that is, $\mathbf{A}^{\pm}(\mathbf{x})$ and $\sigma^{\pm}(\mathbf{x})$, are function of $\mathbf{x}$ but may have finite jumps at the interface, then the last three identities need to be revised in Theorem 3.1, see Appendix.

3.2. The maximum principle preserving discretization of the PDE at irregular grid points

For an irregular grid point (x_i, y_j, z_k), we want to construct a discrete maximum principle preserving finite difference equation with the following form

$$
\sum_{m=1}^{N_s} \gamma_{ijk,m} U_{i+i_m,j+j_m,k+k_m} + \sigma_{ijk} U_{ijk} = f_{ijk} + C_{ijk}, \tag{3.22}
$$

where i_m, j_m, k_m take values in the set $\{-1, 0, 1\}$. N_s is the number of grid points involved in the discretization, and we often choose $N_s = 27$ in 3D cases; C_{ijk} is a correction term depending on the jump conditions of the solution and the flux. The idea and procedure are similar to the maximum principle preserving scheme [15, 16] for isotropic elliptic interface problems and the FE-FD method [8] for 2D anisotropic elliptic interface problems while the interface relations and the implementation are more challenging.

The local truncation error of the scheme at a grid point (x_i, y_j, z_k) is

$$
T_{ijk} = \sum_{m=1}^{N_s} \gamma_{ijk,m} u(x_{i+i_m}, y_{j+j_m}, z_{k+k_m}) + \sigma_{ijk} u(x_i, y_j, z_k) - f(x_i, y_j, z_k) - C_{ijk}. \tag{3.23}
$$

We describe the process to determine the coefficients of the difference equation (3.22) below. Without of loss of generality, let $(x_i, y_j, z_k) \in \Omega^-$. We first choose a point (X_i^*, Y_j^*, Z_k^*) on the interface Γ near the grid point (x_i, y_j, z_k), say the orthogonal projection of (x_i, y_j, z_k) on the interface. Then we expand each $u(x_{i+i_m}, y_{j+j_m}, z_{k+k_m})$ at (X_i^*, Y_j^*, Z_k^*) under the local coordinate system,

$$
\begin{aligned}
&u(x_{i+i_m}, y_{j+j_m}, z_{k+k_m}) \\
&= u(\xi_m, \eta_m, \tau_m) = u^{\pm} + \xi_m u_\xi^{\pm} + \eta_m u_\eta^{\pm} + \tau_m u_\tau^{\pm} + \frac{1}{2}\xi_m^2 u_{\xi\xi}^{\pm} + \frac{1}{2}\eta_m^2 u_{\eta\eta}^{\pm} \\
&\quad + \frac{1}{2}\tau_m^2 u_{\tau\tau}^{\pm} + \xi_m \eta_m u_{\xi\eta}^{\pm} + \xi_m \tau_m u_{\xi\tau}^{\pm} + \eta_m \tau_m u_{\eta\tau}^{\pm} + O(h^3),
\end{aligned}
\tag{3.24}
$$

where the '+' or '$-$' sign depends on which side the grid point (ξ_m, η_m, τ_m) lies on the interface Γ. With the expansions of all $u(x_{i+i_m}, y_{j+j_m}, z_{k+k_m})$, along with

$$f_{ij} = f^- + O(h), \qquad \sigma_{ij} = \sigma^- + O(h), \tag{3.25}$$

the local truncation error T_{ijk} can be expressed as a linear combination of the values $u^\pm$, $u_\xi^\pm$, $u_\eta^\pm$, $u_\tau^\pm$, $u_{\xi\xi}^\pm$, $u_{\eta\eta}^\pm$, $u_{\tau\tau}^\pm$, $u_{\xi\eta}^\pm$, $u_{\xi\tau}^\pm$, $u_{\eta\tau}^\pm$ as the following:

$$
\begin{aligned}
T_{ijk} =\, & b_1 u^- + b_2 u^+ + b_3 u_\xi^- + b_4 u_\xi^+ + b_5 u_\eta^- + b_6 u_\eta^+ + b_7 u_\tau^- + b_8 u_\tau^+ \\
& + b_9 u_{\xi\xi}^- + b_{10} u_{\xi\xi}^+ + b_{11} u_{\eta\eta}^- + b_{12} u_{\eta\eta}^+ + b_{13} u_{\tau\tau}^- + b_{14} u_{\tau\tau}^+ \\
& + b_{15} u_{\xi\eta}^- + b_{16} u_{\xi\eta}^+ + b_{17} u_{\xi\tau}^- + b_{18} u_{\xi\tau}^+ + b_{19} u_{\eta\tau}^- + b_{20} u_{\eta\tau}^+ \\
& + \sigma^- u^- - f^- - C_{ijk} + O(h).
\end{aligned}
\tag{3.26}
$$

Define two index sets K^+ and K^- by

$$K^\pm = \left\{ m : (\xi_m, \eta_m, \tau_m) \in \Omega^\pm \right\},$$

then b_j's are given by

$$
\begin{aligned}
& b_1 = \sum_{m \in K^-} \gamma_{ijk,m}, && b_2 = \sum_{m \in K^+} \gamma_{ijk,m}, && b_3 = \sum_{m \in K^-} \xi_m \gamma_{ijk,m}, \\
& b_4 = \sum_{m \in K^+} \xi_m \gamma_{ijk,m}, && b_5 = \sum_{m \in K^-} \eta_m \gamma_{ijk,m}, && b_6 = \sum_{m \in K^+} \eta_m \gamma_{ijk,m}, \\
& b_7 = \sum_{m \in K^-} \tau_m \gamma_{ijk,m}, && b_8 = \sum_{m \in K^+} \tau_m \gamma_{ijk,m}, && b_9 = \frac{1}{2} \sum_{m \in K^-} \xi_m^2 \gamma_{ijk,m}, \\
& b_{10} = \frac{1}{2} \sum_{m \in K^+} \xi_m^2 \gamma_{ijk,m}, && b_{11} = \frac{1}{2} \sum_{m \in K^-} \eta_m^2 \gamma_{ijk,m}, && b_{12} = \frac{1}{2} \sum_{m \in K^+} \eta_m^2 \gamma_{ijk,m}, \\
& b_{13} = \frac{1}{2} \sum_{m \in K^-} \tau_m^2 \gamma_{ijk,m}, && b_{14} = \frac{1}{2} \sum_{m \in K^+} \tau_m^2 \gamma_{ijk,m}, && b_{15} = \sum_{m \in K^-} \xi_m \eta_m \gamma_{ijk,m}, \\
& b_{16} = \sum_{m \in K^+} \xi_m \eta_m \gamma_{ijk,m}, && b_{17} = \sum_{m \in K^-} \xi_m \tau_m \gamma_{ijk,m}, && b_{18} = \sum_{m \in K^+} \xi_m \tau_m \gamma_{ijk,m}, \\
& b_{19} = \sum_{m \in K^-} \eta_m \tau_m \gamma_{ijk,m}, && b_{20} = \sum_{m \in K^+} \eta_m \tau_m \gamma_{ijk,m}.
\end{aligned}
\tag{3.27}
$$

Using ten interface relations defined in Theorem 3.1, we eliminate the quantities from the '+' side by the quantities from the '$-$' side, and collect terms to obtain

$$
\begin{aligned}
T_{ijk} =\, & B_1 u^- + B_2 u_\xi^- + B_3 u_\eta^- + B_4 u_\tau^- + B_5 u_{\xi\xi}^- + B_6 u_{\eta\eta}^- + B_7 u_{\tau\tau}^- + B_8 u_{\xi\eta}^- \\
& + B_9 u_{\xi\tau}^- + B_{10} u_{\eta\tau}^- + \sigma^- u^- - f^- + B_{11} - C_{ijk} + O(h),
\end{aligned}
\tag{3.28}
$$

where

$$B_1 = b_1 + b_2 + b_{10}\frac{[\sigma]}{a_{11}^+},$$

$$B_2 = b_3 + b_4\frac{a_{11}^-}{a_{11}^+} + S_{m7}[a_{11}] + b_{16}S_{m1} + b_{18}S_{m2} + b_{10}C_{1,1},$$

$$B_3 = b_5 + b_6 - b_4\frac{[a_{12}]}{a_{11}^+} + S_{m7}[a_{12}] + b_{16}S_{m3} + b_{18}S_{m4} + b_{10}C_{1,2},$$

$$B_4 = b_7 + b_8 - b_4\frac{[a_{13}]}{a_{11}^+} + S_{m7}[a_{13}] + b_{16}S_{m5} + b_{18}S_{m6} + b_{10}C_{1,3},$$

$$B_5 = b_9 + b_{10}\frac{a_{11}^-}{a_{11}^+},$$

$$B_6 = b_{11} + b_{12} - b_{16}\frac{[a_{12}]}{a_{11}^+} + b_{10}\frac{2a_{12}^+[a_{12}] - a_{11}^+[a_{22}]}{(a_{11}^+)^2},$$

$$B_7 = b_{13} + b_{14} - b_{18}\frac{[a_{13}]}{a_{11}^+} + b_{10}\frac{2a_{13}^+[a_{13}] - a_{11}^+[a_{33}]}{(a_{11}^+)^2},$$

$$B_8 = b_{15} + b_{16}\frac{a_{11}^-}{a_{11}^+} + b_{10}\frac{2\left(a_{11}^+a_{12}^- - a_{11}^-a_{12}^+\right)}{(a_{11}^+)^2},$$

$$B_9 = b_{17} + b_{18}\frac{a_{11}^-}{a_{11}^+} + b_{10}\frac{2\left(a_{11}^+a_{13}^- - a_{11}^-a_{13}^+\right)}{\left(a_{11}^+\right)^2},$$

$$B_{10} = b_{19} + b_{20}\frac{a_{11}^-}{a_{11}^+} - b_{16}\frac{[a_{13}]}{a_{11}^+} - b_{18}\frac{[a_{12}]}{a_{11}^+} + b_{10}\frac{2\left(a_{12}^+[a_{13}] + a_{13}^+[a_{12}] - a_{11}^+[a_{23}]\right)}{\left(a_{11}^+\right)^2},$$

$$B_{11} = \left(b_2 + b_{10}\frac{\sigma^+}{a_{11}^+}\right)w + \left\{b_6 - b_4\frac{a_{12}^+}{a_{11}^+} + S_{m7}a_{12}^+ + b_{16}S_{n1} + b_{18}S_{n2} + b_{10}C_{1,4}\right\}w_\eta$$

$$+ \left\{b_8 - b_4\frac{a_{13}^+}{a_{11}^+} + S_{m7}a_{13}^+ + b_{16}S_{n3} + b_{18}S_{n4} + b_{10}C_{1,5}\right\}w_\tau$$

$$+ \left\{b_{12} - b_{16}\frac{a_{12}^+}{a_{11}^+} + b_{10}\frac{2(a_{12}^+)^2 - a_{11}^+a_{22}^+}{(a_{11}^+)^2}\right\}w_{\eta\eta}$$

$$+ \left\{b_{14} - b_{18}\frac{a_{13}^+}{a_{11}^+} + b_{10}\frac{2(a_{13}^+)^2 - a_{11}^+a_{33}^+}{(a_{11}^+)^2}\right\}w_{\tau\tau}$$

$$+ \left\{b_{20} - b_{16}\frac{a_{13}^+}{a_{11}^+} - b_{18}\frac{a_{12}^+}{a_{11}^+} + b_{10}\frac{2(2a_{12}^+a_{13}^+ - a_{11}^+a_{23}^+)}{(a_{11}^+)^2}\right\}w_{\eta\tau}$$

$$+ \left\{\frac{b_4}{a_{11}^+} - S_{m7} + b_{16}S_{n5} + b_{18}S_{n6} + b_{10}C_{1,6}\right\}Q$$

$$+ \frac{1}{(a_{11}^+)^2}\left\{b_{16}a_{11}^+ - 2b_{10}a_{12}^+\right\}Q_\eta + \frac{1}{(a_{11}^+)^2}\left\{b_{18}a_{11}^+ - 2b_{10}a_{13}^+\right\}Q_\tau - b_{10}\frac{[f]}{a_{11}^+}.$$

The finite difference coefficients should be determined to have $O(h)$ the local truncation error, and to have an M-matrix structure for the convergence proof. So the coefficients $\gamma_{ijk,m}$ are chosen such that the coefficients of $u^-, u_\xi^-, u_\eta^-, u_\tau^-, u_{\xi\xi}^-, u_{\eta\eta}^-, u_{\tau\tau}^-, u_{\xi\eta}^-, u_{\xi\tau}^-, u_{\eta\tau}^-$ vanish in the local

truncation error (3.28) and satisfy the sigh constraints. In other words, the finite difference coefficients $\gamma_{ijk,m}$ should satisfy the following equality constraints

$$B_1 = 0, \quad B_2 = 0, \quad B_3 = 0, \quad B_4 = 0, \quad B_5 = a_{11},$$

$$B_6 = a_{22}, \ B_7 = a_{33}, \ B_8 = a_{12}, \ B_9 = a_{13}, \ B_{10} = a_{23},$$

$$(3.29)$$

and inequality constraints

$$-\frac{C}{h^2} \le \gamma_{ijk,m} \le 0 \qquad \text{if} \ \ (i_m, j_m, k_m) \ne (0,0,0),$$

$$0 < \gamma_{ijk,m} \le \frac{C}{h^2} \qquad \text{if} \ \ (i_m, j_m, k_m) = (0,0,0),$$

$$(3.30)$$

where C is a positive constant, and $B_j, j = 1, 2, \cdots, 11$ are defined in (3.28). Moreover, to ensure the local truncation errors in (3.28) are bounded by $O(h)$, we should choose the correction terms as $C_{ijk} = B_{11}$.

This equality and inequality constraints are formulated as a quadratic optimization problem,

$$\min_\gamma \left\{ \frac{1}{2} \|\gamma - g\|_2^2 \right\},$$

$$(3.31)$$

such that the equality constraints (3.29) and the inequality constraints (3.30) are satisfied, where $g \in R^{N_s}$ and γ is a vector consisted by finite difference coefficients $\gamma_{ijk,m}$. The vector g in (3.31) is chosen in such a way that if the anisotropic coefficients $\mathbf{A}^+ = \mathbf{A}^-$, the coefficients $\gamma_{ijk,m}$'s are the same or close to the regular ones derived in section 2. For example, when $\mathbf{A}^\pm$ are two piecewise constant matrices, the vector g is chosen as

$$g_m = -\frac{6A_{11}^\pm + 6A_{22}^\pm + 6A_{33}^\pm - 4A_{12}^\pm - 4A_{13}^\pm - 4A_{23}^\pm}{3h^2} \qquad \text{if} \ \ (i_m, j_m, k_m) = (0,0,0),$$

$$g_m = \frac{A_{12}^\pm + A_{13}^\pm + A_{23}^\pm}{3h^2} \qquad \text{if} \ \ (i_m, j_m, k_m) \in \{(-1,-1,-1),(1,1,1)\},$$

$$g_m = -\frac{-3A_{11}^\pm + 2A_{12}^\pm + 2A_{13}^\pm - A_{23}}{3h^2} \qquad \text{if} \ \ (i_m, j_m, k_m) \in \{(-1,0,0),(1,0,0)\},$$

$$g_m = -\frac{-3A_{22}^\pm + 2A_{12}^\pm - A_{13}^\pm + 2A_{23}^\pm}{3h^2} \qquad \text{if} \ \ (i_m, j_m, k_m) \in \{(0,-1,0),(0,1,0)\},$$

$$g_m = -\frac{-3A_{33}^\pm - A_{12}^\pm + 2A_{13}^\pm + 2A_{23}^\pm}{3h^2} \qquad \text{if} \ \ (i_m, j_m, k_m) \in \{(0,0,-1),(0,0,1)\},$$

$$g_m = -\frac{-2A_{12}^\pm + A_{13}^\pm + A_{23}^\pm}{3h^2} \qquad \text{if} \ \ (i_m, j_m, k_m) \in \{(-1,-1,0),(1,1,0)\},$$

$$g_m = -\frac{A_{12}^\pm - 2A_{13}^\pm + A_{23}^\pm}{3h^2} \qquad \text{if} \ \ (i_m, j_m, k_m) \in \{(-1,0,-1),(1,0,1)\},$$

$$g_m = -\frac{A_{12}^\pm + A_{13}^\pm - 2A_{23}^\pm}{3h^2} \qquad \text{if} \ \ (i_m, j_m, k_m) \in \{(0,-1,-1),(0,1,1)\},$$

$$(3.32)$$

where the sign '$\pm$' depends on which side of the interface the grid point $(x_{i+i_m}, y_{j+j_m}, z_{k+k_m})$ lied on.

From [15,16], we know that the optimization problem (3.31) has a solution if h is sufficiently small, which is demonstrated numerically. We use the QL code developed by Schittkowski [17] to solve the optimization problem. Once the $\gamma_{ijk,m}$'s are determined, we get the correction term $C_{ijk} = B_{11}$. If there is no feasible solution for optimization problem, we can add more grid

points nearby until we get a feasible solution. Another way is to use a scaling (preconditioning) strategy which works well, see Example 4.6 as an illustration.

Remark 3.2. If the coefficient matrix $\mathbf{A}$ is a piecewise variable matrix and σ is a piecewise variable function, then B_2, B_3, B_4 and B_{11} become,

$$
\begin{cases}
\widetilde{B}_2 = B_2 + b_{10}\dfrac{a_{11}^+ c_1^- - a_{11}^- c_1^+}{(a_{11}^+)^2}, \\[2mm]
\widetilde{B}_3 = B_3 + b_{10}\dfrac{c_1^+[a_{12}] - a_{11}^+[c_2]}{(a_{11}^+)^2}, \\[2mm]
\widetilde{B}_4 = B_4 + b_{10}\dfrac{c_1^+[a_{13}] - a_{11}^+[c_3]}{(a_{11}^+)^2}, \\[2mm]
\widetilde{B}_{11} = B_{11} + b_{10}\dfrac{a_{12}^+ c_1^+ - a_{11}^+ c_2^+}{(a_{11}^+)^2}w_\eta + b_{10}\dfrac{a_{13}^+ c_1^+ - a_{11}^+ c_3^+}{(a_{11}^+)^2}w_\tau - \dfrac{c_1^+}{(a_{11}^+)^2}Q.
\end{cases}
\tag{3.33}
$$

3.3. The convergence analysis

We show that the proposed new method for 3D anisotropic elliptic interface problems is second order convergent except for a factor of $|\log h|^{4/3}|$ in the pointwise norm.

Theorem 3.2. *Let $u(x,y,z) \in C^3(\Omega^\pm)$ be the solution of problems* (1.1)–(1.4) *with $\sigma(\mathbf{x}) = 0$, a Dirichlet boundary condition. Assume that $\partial\Omega$ is Lipschitz continuous, the interface is smooth ($\varphi(x,y,z) \in C^2$), $\mathbf{A}$ is a symmetric positive definite and piecewise constant matrix, and the finite difference coefficients $\{\gamma_{ijk,m}\}$ at irregular grid points satisfy*

$$
\sum_{\xi_m \geq 0} \gamma_{ijk,m}\xi_m \geq \frac{C_2}{h},
\tag{3.34}
$$

where C_2 is a positive constant that corresponds to the source strength of the singular source term, corresponding to the magnitude of the flux jump condition, that is, $\|Q\|_{\infty,\Gamma}$. The flux jump condition $[\mathbf{A}u_n] = Q$ corresponds to a source distribution along the interface (single layer as in Peskin's Immersed Boundary Method) model. In the discretization, the right hand side will have $O(1/h)$ terms at nodal points near the interface. Thus, the condition is actually a consistency requirement, see for example, [15] for more details. Then we have the following error estimate for the computed solution U_{ijk} of the proposed method,

$$
\max_{ijk} |u(x_i, y_j, z_k) - U_{ijk}| \leq C|\log h|^{4/3}h^2,
\tag{3.35}
$$

where the constant C depends on the underlined grid, interface, u, f, and $\mathbf{A} = \{a_{ij}\}$, and the space $C^k(\Omega^\pm)$ are defined as

$$
C^k(\Omega^\pm) = \{v(\mathbf{x}) | v(\mathbf{x})|_{\mathbf{x}\in\Omega^+} \in C^k(\Omega^+), v(\mathbf{x})|_{\mathbf{x}\in\Omega^-} \in C^k(\Omega^-)\}, \quad k = 1, 2, 3, \cdots.
$$

We remark that the condition (3.34)is a consistency condition for the maximum principle preserving scheme, which states that finite difference coefficients should be non-negative and bounded by C/h^2, at least one of them should be $O(1/h^2)$.

Proof. The proof is similar to the process of 2D anisotropic elliptic interface problems in [8]. We divide the error into three parts and analyze them separately. Let the discrete matrix of the FE-FD scheme be $\mathbf{K}_h$, and the error vector of the computed solution be $\mathbf{E}_h$, then we have

$$\mathbf{K}_h \mathbf{E}_h = \mathbf{T}_h = \mathbf{T}_h^+ + \mathbf{T}_h^\Gamma + \mathbf{T}_h^-, \tag{3.36}$$

where entries of $\mathbf{T}_h^+$ are the local truncation errors of the new finite difference scheme at regular grid points in Ω^+, and are zeros at regular grid points in Ω^-, and irregular grid points in the neighborhood of Γ and so on.

We define $\mathbf{K}_h^+$ as the finite difference (from FEM) operator on the entire domain with the anisotropic coefficient matrix $\mathbf{A}^+$ defined on Ω^+, that is extended to the entire domain since $\mathbf{A}^+$ is a constant matrix. $\mathbf{K}_h^-$ is defined in the same way. $\mathbf{K}_h^+$ and $\mathbf{K}_h^-$ are symmetric positive definite matrices. Note also that since $\mathbf{A}$ is a piecewise constant matrix, the discrete matrix $\mathbf{K}_h^+$ and $\mathbf{K}_h^-$ are exact. The error in approximating the load vector is of $O(h^2)$, which has the same order as that of the local truncation errors. Finally, we define $\mathbf{K}_h^\Gamma$ as an extension of the maximum preserving finite difference scheme at irregular grid points to all grid points. Note that $\mathbf{K}_h^\Gamma$ is a second order finite difference operator at regular grid points and it is an M-matrix if it would be applied to a non-interface problem. Note also that the extension is used for the theoretical purpose but not for the computational practice since it would be computational expensive.

If we define $\mathbf{E}_h^+$, $\mathbf{E}_h^-$, and $\mathbf{E}_h^\Gamma$ in the same way as their counter-parts by replacing T with E, then

$$\mathbf{E}_h = \mathbf{E}_h^+ + \mathbf{E}_h^\Gamma + \mathbf{E}_h^- = \left(\mathbf{K}_h^+\right)^{-1} \mathbf{T}_h^+ + \left(\mathbf{K}_h^\Gamma\right)^{-1} \mathbf{T}_h^\Gamma + \left(\mathbf{K}_h^-\right)^{-1} \mathbf{T}_h^-. \tag{3.37}$$

We show below that each term in the right hand side is bounded by $O(h^2)$ or $O(|\log h|^{4/3} h^2)$.

The first term corresponds to the error estimate of the following problem

$$-\nabla \cdot \left(\mathbf{A}^+(\mathbf{x}) \nabla q(\mathbf{x})\right) = \begin{cases} T_f^+(\mathbf{x}) & \text{if } \mathbf{x} \in \Omega^+, \\ 0 & \text{otherwise,} \end{cases} \qquad q\Big|_{\partial\Omega} = 0,$$

where

$$T_f^+(\mathbf{x}) = \sum_{\mathbf{x}_m \in \Omega^+} T_m \, \psi_m(\mathbf{x}), \qquad \text{and thus,} \qquad \|T_f^+\|_{L^\infty} \leq Ch^2,$$

and T_m is the local truncation error at a regular nodal point $\mathbf{x}_m$ in (2.18). Note that this is an anisotropic elliptic problem with smooth coefficients but a L^2 source term with a finite discontinuity.

We show that $q \in W^{2,\infty}(\Omega)$ below. As a matter of fact, $q(\mathbf{x})$ is piecewise smooth, see for example [18], in particular,

$$q(\mathbf{x})|_{\Omega^\pm} \in C^2(\bar{\Omega}^\pm).$$

Define $p(\mathbf{x})$ by

$$p(\mathbf{x})|_{\Omega^\pm} = \left(q(\mathbf{x})|_{\Omega^\pm} \right)_{xx}.$$

Then $p(\mathbf{x}) \in L^\infty(\Omega)$. It can be shown as following that $p(\mathbf{x})$ is the weak second derivative of $q(\mathbf{x})$ with respect to x. For any $\varphi \in C_0^\infty(\Omega)$,

$$\int_\Omega p\varphi \, d\mathbf{x} = \sum_{i=1}^2 \int_{\Omega_i} q_{xx}\varphi \, d\mathbf{x} = -\sum_{i=1}^2 \left(\int_{\Omega_i} q_x\varphi_x \, d\mathbf{x} - \int_{\partial\Omega_i} q_x\varphi n_x \, ds \right)$$

$$= -\sum_{i=1}^2 \left(-\int_{\Omega_i} q\varphi_{xx} \, d\mathbf{x} + \int_{\partial\Omega_i} q\varphi_x n_x ds - \int_{\partial\Omega_i} q_x\varphi n_x \, ds \right)$$

$$= \int_\Omega q\varphi_{xx} \, d\mathbf{x} + \int_\Gamma \left(-[q\varphi_x n_x^\Gamma] + [q_x\varphi n_x^\Gamma] \right) ds = \int_\Omega q\varphi_{xx} \, d\mathbf{x},$$

where $\Omega_1 = \Omega^+$, $\Omega_2 = \Omega^-$, (n_x, n_y, n_z) is the normal direction of $\partial\Omega$, $(n_x^\Gamma, n_y^\Gamma, n_z^\Gamma)$ is the normal direction of Γ. We have used the fact that $q(\mathbf{x}) \in C^1(\bar\Omega)$ in deriving the last identity. Therefore, $q_{xx} = p \in L^\infty(\Omega)$. Similarly, $q_{yy}, q_{zz}, q_{xy}, q_{xz}, q_{yz} \in L^\infty(\Omega)$. As a consequence, $q \in W^{2,\infty}(\Omega)$. Note also that when $\sigma(\mathbf{x}) = 0$ and $\mathbf{A}$ is a constant matrix, we can change the regular anisotropic PDE to a Poisson equation without alter the regularity. Thus, the finite element discretization using P_1 element satisfies the following estimate from [13, 14],

$$\|\mathbf{E}_h^+\|_\infty \le C|\log h|^{4/3}\|q\|_{W^{2,\infty}(\Omega)} \le Ch^2|\log h|^{4/3}\|u\|_{W^{2,\infty}(\Omega)}.$$

We can get the same order estimate for $\|\mathbf{E}_h^-\|_\infty$.

Finally, we prove the error estimate for $\mathbf{E}_h^\Gamma$. The proof is similar to the maximum preserving IIM [16] for the scaler case. Consider the solution to the following interface problem

$$\begin{cases} -\nabla \cdot (\mathbf{A}\nabla\phi(\mathbf{x})) + \sigma\phi(\mathbf{x}) = 1, \\ [\phi] = 0, \quad [\mathbf{A}\nabla\phi \cdot \mathbf{n}] = 1, \quad \phi_{\partial\Omega} = 1. \end{cases} \tag{3.38}$$

From the results in [18], we know that the solution ϕ exists, and it is unique and piecewise smooth. Therefore the solution is also bounded. Let

$$\bar\phi(x, y, z) = \phi(x, y, z) + \left| \min_{(x,y,z)\in\Omega} \phi(x, y, z) \right|. \tag{3.39}$$

Note that the second term in the right hand side is a constant. If (3.34) is true, then we know that

$$\mathbf{B}_h^\Gamma \bar\phi(x_i, y_j, z_k) \ge \begin{cases} 1 + O(h^2), & \text{if } (x_i, y_j, z_k) \text{ is a regular grid point}, \\ \displaystyle\sum_{\xi_m \ge 0} \gamma_m \xi_m \ge \frac{C_2}{h} + O(1), & \text{if } (x_i, y_j, z_k) \text{ is an irregular grid point.} \end{cases}$$

Note that the second inequality above is due to the jump in the flux in $\bar\phi$ at irregular grid points; and $\mathbf{B}_h^\Gamma \bar\phi(x_i, y_j, z_k)$ can be large but it is nonnegative. At regular grid points we have

$$\frac{|T_{ijk}|}{\mathbf{B}_h^\Gamma \bar\phi(x_i, y_j, z_k)} \le \frac{C_3 h^2}{1},$$

where T_{ijk} is the local truncation error if we would apply $\mathbf{B}_h^\Gamma$ to the original PDE at a regular grid point $\mathbf{x}_m = (x_i, y_j, z_k)$. At irregular grid points where (3.34) is satisfied, we have

$$\frac{|T_{ijk}|}{\mathbf{B}_h^\Gamma \bar\phi(x_i, y_j, z_k)} \le \frac{C_4 h}{C_2/h}, = \frac{C_4}{C_2}h^2$$

since the local truncation errors at irregular grid points are bounded by

$$|T_{ijk}| \leq C_4 h$$

for some constant C_4. Thus, from Theorem 6.2 in [19], we also have $\|\mathbf{E}_h^\Gamma\|_\infty \leq Ch^2$. This completes the proof. □

Remark 3.3. We believe that the convergence theorem is also true for variable coefficient matrix $\mathbf{A}$ and non-zero $\sigma(\mathbf{x})$ at least asymptotically. This is because at regular grid points, the differences of the computed coefficient matrix $\mathbf{A}_h$ and the exact one using the P_1 finite element method is order of $O(h^2)$.

4. Numerical Experiments

In this section, we show several numerical experiments for the 3D anisotropic elliptic interface problems with piecewise constant and variable anisotropic coefficients respectively. The discrete linear system of equations is solved using SOR. The interface are some closed surface in the solution domain and are expressed by a level set function. We present errors in the solution denoted as $\|E_N\|_\infty$ in the infinity norm,

$$\|E_N\|_\infty = \max_{ijk} |u(x_i, y_j, z_k) - U_{ijk}|.$$

Table 4.1: A grid refinement analysis for Example 4.1 with two modest jumps in the coefficients.

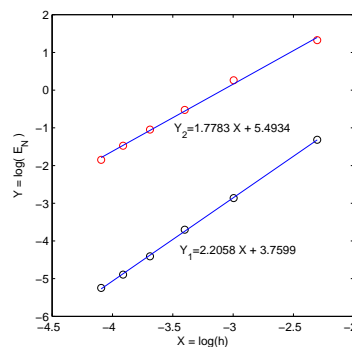| N	$\max\limits_{i,j}\left\{\dfrac{\|A_{ij}^+\|}{\|A_{ij}^-\|}\right\} = 30$	$\max\limits_{i,j}\left\{\dfrac{\|A_{ij}^+\|}{\|A_{ij}^-\|}\right\} = 1/20$
	$\|E_N\|_\infty$	$\|E_N\|_\infty$
20	2.6821E-01	3.7643E+00
40	5.7095E-02	1.2981E+00
60	2.4670E-02	5.9125E-01
80	1.2182E-02	3.5124E-01
100	7.5081E-03	2.2920E-01
120	5.2703E-03	1.5735E-01

Fig. 4.1. Linear regression of Table 4.1. The average convergence orders are 2.2058 and 1.7783, respectively.

Table 4.2: A grid refinement analysis for Example 4.1 with two large jumps in the coefficients.

N	$\max\limits_{i,j}\left\{\frac{\|A_{ij}^+\|}{\|A_{ij}^-\|}\right\} = 4000$	$\max\limits_{i,j}\left\{\frac{\|A_{ij}^+\|}{\|A_{ij}^-\|}\right\} = 30000$
	$\|E_N\|_\infty$	$\|E_N\|_\infty$
20	2.5033E-01	2.4788E-01
40	4.9835E-02	4.9069E-02
60	2.0528E-02	2.0032E-02
80	9.6391E-03	9.3921E-03
100	5.8327E-03	5.6424E-03
120	4.0188E-03	3.8821E-03

The order of convergence is estimated using the linear regression from the datas $\log(E_N)$ and $\log(h_N)$ with different N' s.

To simplify the expression, we rewrite the coefficient matrix $\mathbf{A}$ as $(A_{11}, A_{22}, A_{33}, A_{12}, A_{13}, A_{23})$. For example, $A^- : A^+ = (4, 5, 7, 0.1, 0.2, 0.3) : (40, 60, 80, 3, 6, 9)$ means

$$\mathbf{A}^- = \begin{pmatrix} 4 & 0.1 & 0.2 \\ 0.1 & 5 & 0.3 \\ 0.2 & 0.3 & 7 \end{pmatrix}, \quad \mathbf{A}^+ = \begin{pmatrix} 40 & 3 & 6 \\ 3 & 60 & 9 \\ 6 & 9 & 80 \end{pmatrix}.$$

Example 4.1. In this example, the anisotropic coefficient $\mathbf{A}$ of differential equation is a piecewise constant matrix. The jumps $[u]$ in the solution, the flux jump condition $[\mathbf{A}u_n]$, $[f]$ in the source term, and the Dirichlet boundary are determined according to the exact solution:

$$u(x, y, z) = \begin{cases} -10\left(x^2 + y^2 + z^2\right)^2 & \text{if } x^2 + y^2 + z^2 < \left(\frac{\pi}{6.28}\right)^2, \\ \left(x^2 + y^2 + z^2\right)^2 & \text{if } x^2 + y^2 + z^2 \geq \left(\frac{\pi}{6.28}\right)^2. \end{cases} \tag{4.1}$$

The interface is a sphere $x^2 + y^2 + z^2 = \left(\frac{\pi}{6.28}\right)^2$ within the computation domain $-1 \leq x, y, z \leq 1$.

In Tables 4.1-4.2, we show grid refinement results to get actual errors in the strongest norm and average convergence order with a modest jump and a large jump in the coefficients $\mathbf{A}$ and σ respectively, along with a convergence plot using a line fitting. In Table 4.1, the second column lists the errors when $A^- : A^+ = (4, 5, 7, 0.1, 0.2, 0.3) : (40, 60, 80, 3, 6, 9)$, $\sigma^- : \sigma^+ = 1 : 10$, while the third column shows the errors when $A^- : A^+ = (60, 40, 50, 10, 15, 20) : (3, 4, 5, 1, 1.5, 2)$, $\sigma^- : \sigma^+ = 10 : 1$. In Table 4.2, the second column lists the errors when $A^- : A^+ = (0.1, 0.2, 0.3, 0.01, 0.02, 0.03) : (200, 600, 300, 40, 60, 90)$, $\sigma^- : \sigma^+ = 0.1 : 100$, while the third column show the errors when $A^- : A^+ = (0.1, 0.2, 0.3, 0.01, 0.02, 0.03) : (3000, 4000, 5000, 200, 600, 900)$, $\sigma^- : \sigma^+ = 0.1 : 1000$. Using the linear regression analysis, we can see a second order convergence in the solution for all cases.

The linear regression analysis corresponding to Table 4.1 in Fig. 4.1 provided the convergence order and error constants below:

$$\| U^h - u \|_\infty \approx 42.9458\, h^{2.2058}, \quad \| U^h - u \|_\infty \approx 243.0901\, h^{1.7783}.$$

The linear regression results corresponding to Table 4.2 in Fig. 4.2 provided the convergence order and error constants below:

$$\| U^h - u \|_\infty \approx 52.7039\, h^{2.3222}, \quad \| U^h - u \|_\infty \approx 54.0428\, h^{2.3366}.$$
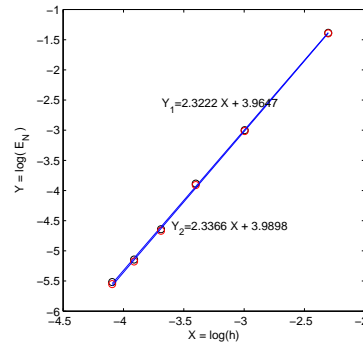
Fig. 4.2. Linear regression of Table 4.2. The average convergence orders are 2.3222 and 2.3366, respectively.

Table 4.3: A grid refinement analysis for Example 4.2 with two modest jumps in the coefficients.

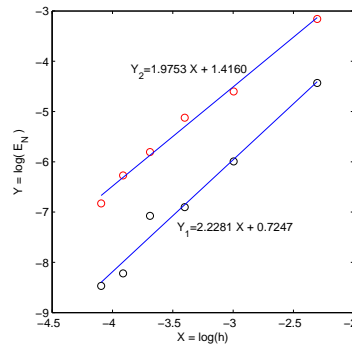| N	$\max\limits_{i,j}\left\{\dfrac{\|A_{ij}^+\|}{\|A_{ij}^-\|}\right\} = 90$	$\max\limits_{i,j}\left\{\dfrac{\|A_{ij}^+\|}{\|A_{ij}^-\|}\right\} = 1/20$
	$\\|E_N\\|_\infty$	$\\|E_N\\|_\infty$
20	1.1902E-02	4.2480E-02
40	2.4935E-03	1.0033E-02
60	1.0046E-03	5.9599E-03
80	8.4603E-04	3.0099E-03
100	2.6913E-04	1.8888E-03
120	2.0980E-04	1.0829E-03

Fig. 4.3. Linear regression of Table 4.3. The average convergence orders are 2.2281 and 1.9753, respectively.

Example 4.2. In the second example, we also select the anisotropic coefficient $\mathbf{A}$ as a piecewise constant matrix and σ is a piecewise constant, while the interface is a ellipsoid $x^2+4y^2+2z^2 = \frac{1}{4}$ within the computation domain $-1 \leq x, y, z \leq 1$. The jumps $[u]$, $[\mathbf{A}u_n]$, $[f]$, and the Dirichlet boundary condition are determined from the exact solution:

$$u(x,y,z) = \begin{cases} x^2 - y^2 - z^2 & \text{if } x^2 + 4y^2 + 2z^2 < \dfrac{1}{4}, \\ \sin(x)\cos(y)\cos(z) & \text{if } x^2 + 4y^2 + 2z^2 \geq \dfrac{1}{4}. \end{cases} \qquad (4.2)$$

Table 4.4: A grid refinement analysis for Example 4.2 with two large jumps in the coefficients.

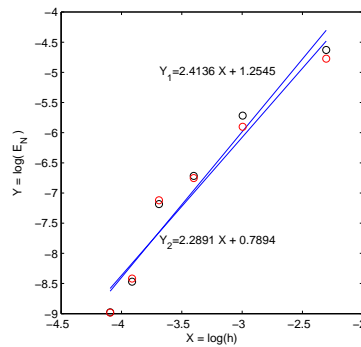| N	$\max\limits_{i,j}\left\{\frac{|A^+_{ij}|}{|A^-_{ij}|}\right\} = 9000$	$\max\limits_{i,j}\left\{\frac{|A^+_{ij}|}{|A^-_{ij}|}\right\} = 100000$
	$\|E_N\|_\infty$	$\|E_N\|_\infty$
20	9.7614E-03	8.4578E-03
40	3.2877E-03	2.7341E-03
60	1.2099E-03	1.1676E-03
80	7.5818E-04	8.0835E-04
100	2.0947E-04	2.2079E-04
120	1.2624E-04	1.2555E-04

Fig. 4.4. Linear regression of Table 4.4. The average convergence orders are 2.4136 and 2.2891, respectively.

The grid refinement results presented in Tables 4.3-4.4 with a modest jump and a large jump in the coefficients $\mathbf{A}$ and σ show a second order convergence in the solution. In Table 4.3, the second column lists the errors when $A^- : A^+ = (4,5,7,0.1,0.2,0.3) : (80,60,70,9,6,5)$, $\sigma^- : \sigma^+ = 1 : 10$, while the third column shows the errors when $A^- : A^+ = (60,40,50,-10,-5,-2) : (3,4,5,-1,-0.5,-0.2)$, $\sigma^- : \sigma^+ = 10 : 1$. In Table 4.4, the second column lists the errors when $A^- : A^+ = (4,6,5,1,0.5,0.1) : (4000,6000,5000,1000,500,900)$, $\sigma^- : \sigma^+ = 1 : 5000$, while the third column shows the errors when $A^- : A^+ = (0.1,0.2,0.3,0.01,0.02,0.03) : (4000,6000,5000,1000,500,900)$, $\sigma^- : \sigma^+ = 0.1 : 2000$.

The linear regression results corresponding to Table 4.3 in Fig. 4.3 provided the convergence order and error constants below:

$$\| U^h - u \|_\infty \approx 2.0640\, h^{2.2281}, \qquad \| U^h - u \|_\infty \approx 4.1205\, h^{1.9753}.$$

The linear regression results corresponding to Table 4.4 in Fig. 4.4 provided the convergence order and error constants below:

$$\| U^h - u \|_\infty \approx 3.5060\, h^{2.4136}, \qquad \| U^h - u \|_\infty \approx 2.2020\, h^{2.2891}.$$

Example 4.3. In this example, we set the domain as a multi-connected domain with two ellipsoid interfaces. The level set function of the interface is

$$\varphi(x,y,z) = S_1(x,y,z)S_2(x,y,z),$$

Table 4.5: A grid refinement analysis for Example 4.3 with two modest jumps in the coefficients.

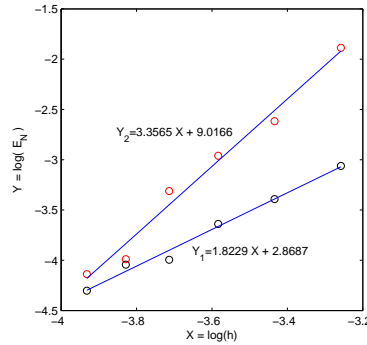| N	$\max\limits_{i,j}\left\{\frac{|A_{ij}^+|}{|A_{ij}^-|}\right\} = 30$	$\max\limits_{i,j}\left\{\frac{|A_{ij}^+|}{|A_{ij}^-|}\right\} = 1/10$
	$\|E_N\|_\infty$	$\|E_N\|_\infty$
52	4.6789E-02	1.5159E-01
62	3.3652E-02	7.3042E-02
72	2.6281E-02	5.1766E-02
82	1.8408E-02	3.6438E-02
92	1.7532E-02	1.8517E-02
102	1.3532E-02	1.5956E-02

Fig. 4.5. Linear regression of Table 4.5. The average convergence orders are 1.8229 and 3.3565, respectively.

where

$$S_1(x,y,z) = (x - 0.2)^2 + 2(y - 0.2)^2 + z^2 - 0.01,$$
$$S_2(x,y,z) = 2(x + 0.2)^2 + (y + 0.2)^2 + z^2 - 0.01.$$

The anisotropic coefficient $\mathbf{A}$ and σ are still piecewise constant. The jumps $[u]$, $[\mathbf{A}u_n]$, $[f]$ and the Dirichlet boundary are determined from the following exact solution:

$$u(x,y,z) = \begin{cases} e^{x+2y+z} & \text{if } (x,y,z) \in \Omega^-, \\ \sin(2\pi x) + \sin(\pi y) + \sin(4\pi z) & \text{if } (x,y,z) \in \Omega^+. \end{cases} \tag{4.3}$$

We show a grid refinement results in Tables 4.5-4.6, and by a linear regression analysis we can see a clean second order convergence for both a modest jump and a large jump in the coefficients $\mathbf{A}$ and σ. In Table 4.5, the second column lists the errors when $A^- : A^+ = (4, 5, 6, 1, 0.5, 0.3) : (50, 60, 70, 10, 5, 9)$, $\sigma^- : \sigma^+ = 1 : 10$, while the third column shows the errors when $A^- : A^+ = (6, 4, 2, -0.1, -0.2, -0.3) : (2, 1, 0.2, -0.01, -0.02, -0.03)$, $\sigma^- : \sigma^+ = 1 : 0.1$. In Table 4.6, the second column lists the errors when $A^- : A^+ = (0.1, 0.2, 0.3, 0.01, 0.02, 0.03) : (400, 600, 700, 60, 80, 90)$, $\sigma^- : \sigma^+ = 0.1 : 100$, while the third column shows the errors when $A^- : A^+ = (0.1, 0.2, 0.3, 0.01, 0.02, 0.03) : (1000, 2000, 3000, 100, 200, 300)$, $\sigma^- : \sigma^+ = 0.1 : 1000$.

The linear regression results corresponding to Table 4.5 in Fig. 4.5 provided the convergence order and error constants below:

$$\| U^h - u \|_\infty \approx 17.6148 \, h^{1.8229}, \qquad \| U^h - u \|_\infty \approx 8238.5817 \, h^{3.3565}.$$

The linear regression results corresponding to Table 4.6 in Fig. 4.6 provided the convergence

Table 4.6: A grid refinement analysis for Example 4.3 with two large jumps in the coefficients.

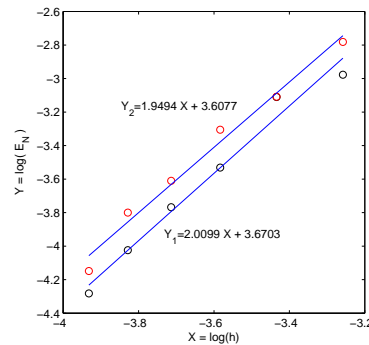| N	$\max\limits_{i,j}\left\{\dfrac{\lvert A_{ij}^{+}\rvert}{\lvert A_{ij}^{-}\rvert}\right\}=6000$	$\max\limits_{i,j}\left\{\dfrac{\lvert A_{ij}^{+}\rvert}{\lvert A_{ij}^{-}\rvert}\right\}=10000$
	$\lVert E_N\rVert_\infty$	$\lVert E_N\rVert_\infty$
20	9.7614E-03	8.4578E-03
40	3.2877E-03	2.7341E-03
60	1.2099E-03	1.1676E-03
80	7.5818E-04	8.0835E-04
100	2.0947E-04	2.2079E-04
120	1.2624E-04	1.2555E-04

Fig. 4.6. Linear regression of Table 4.6. The average convergence orders are 2.0099 and 1.9494, respectively.

order and error constants below:

$$\lVert U^h - u \rVert_\infty \approx 39.2625\, h^{2.0099}, \qquad \lVert U^h - u \rVert_\infty \approx 36.8811\, h^{1.9494}.$$

Example 4.4. In this example, we choose the anisotropic coefficient $\mathbf{A}$ and σ are piecewise variable. $A^-(x,y,z)$ and $A^+(x,y,z)$ are fixed by

$$A^- = \begin{pmatrix} r^2 + 1 & r^2 & r^2 + \frac{1}{5} \\ r^2 & r^2 + 2 & r^2 + \frac{1}{10} \\ r^2 + \frac{1}{5} & r^2 + \frac{1}{10} & r^2 + 3 \end{pmatrix}, \quad A^+ = \beta A^-,$$

and the piecewise variable functions $\sigma^\pm(x,y,z)$ are

$$\sigma^- = e^x \sin y \cos z \left(r^2 + 4\right), \quad \sigma^+ = \beta\sigma^-,$$

Table 4.7: A grid refinement analysis for Example 4.4.

N	$\beta = 1$	$\beta = 2$	$\beta = 1000$
	$\lVert E_N\rVert_\infty$	$\lVert E_N\rVert_\infty$	$\lVert E_N\rVert_\infty$
20	5.4271E-02	2.7686E-02	2.6046E-03
40	1.3710E-02	7.0787E-03	7.2667E-04
60	5.9850E-03	3.1298E-03	3.3120E-04
80	3.3527E-03	1.7622E-03	1.8191E-04
100	2.1525E-03	1.1427E-03	1.1002E-04
120	1.4781E-03	7.7950E-04	8.3248E-05

where β is a constant and $r = \sqrt{x^2 + y^2 + z^2}$. The interface is a sphere $x^2 + y^2 + z^2 = \left(\frac{\pi}{6.28}\right)^2$ within the computation domain $[-1, 1] \times [-1, 1] \times [-1, 1]$. The jump conditions $[u]$ and $[\mathbf{A}u_n]$, the Dirichlet boundary, and the source term f are derived from the following exact solution

$$u(x, y, z) = \begin{cases} r^2 & \text{if } r < r_0, \\ \left(\frac{1}{2}r^4 + r^2\right)/\beta - \left(\frac{1}{2}r_0^4 + r_0^2\right)/\beta + r_0^2 & \text{if } r \geq r_0, \end{cases} \tag{4.4}$$

where $r_0 = \frac{\pi}{6.28}$. We show the grid refinement results in Table 4.7 with three different β. The larger β corresponds to a larger jump in coefficients. From linear regressions, we obtain second order convergence for both a modest and a large jump in the coefficient matrix $\mathbf{A}$ and σ.

The linear regression results corresponding to Table 4.7 in Fig. 4.7 provided the convergence order and error constants below:

$$\| U^h - u \|_\infty \approx 5.6124\, h^{2.0117}, \quad \| U^h - u \|_\infty \approx 2.7234\, h^{1.9901}, \quad \| U^h - u \|_\infty \approx 0.2394\, h^{1.9482}.$$

Example 4.5. We show an example in which the interface is not an ellipsoid. The interface is a perturbed sphere whose curvature can change the signs.

$$x^2 + y^2 + z^2 = \left(C_0 + \epsilon \sin(k_1 x) \sin(k_2 y) \sin(k_3 z)\right)^2. \tag{4.5}$$

The jumps in the solution and the flux, $[u]$ and $[\mathbf{A}u_n]$, $[f]$ in the source term, and the Dirichlet
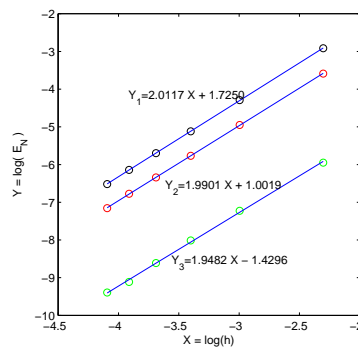

Fig. 4.7. Linear regression of Table 4.7. The average convergence orders are 2.0117, 1.9901, and 1.9482, respectively.

Table 4.8: A grid refinement analysis for Example 4.5 with modest jumps in the coefficients.

N	$\max\limits_{i,j}\left\{\dfrac{\|A_{ij}^+\|}{\|A_{ij}^-\|}\right\} = 10$	$\max\limits_{i,j}\left\{\dfrac{\|A_{ij}^+\|}{\|A_{ij}^-\|}\right\} = 1/10$
	$\|E_N\|_\infty$	$\|E_N\|_\infty$
20	2.0051E-01	1.5930E-01
40	4.5430E-02	3.1351E-02
60	2.0699E-02	1.4232E-02
80	1.1173E-02	7.5786E-03
100	7.2125E-03	5.1957E-03
120	5.0008E-03	3.4735E-03

boundary are determined according to the following exact solution:

$$
u(x, y, z) = \begin{cases} \sin\left(x + 2y + 3z\right) & \text{if } (x, y, z) \in \Omega^-, \\ \left(x^2 + y^2 + z^2\right)^{\frac{7}{2}} & \text{if } (x, y, z) \in \Omega^+. \end{cases} \tag{4.6}
$$

In Table 4.8-4.9, we show grid refinement results followed with the corresponding linear regression of convergence order with $\epsilon = 0.2$, $k_1 = k_2 = k_3 = 5$, $C_0 = 0.5$. In Table 4.8, the second column shows the errors of the computed solutions when $A^- : A^+ = (4, 5, 7, 0.1, 0.2, 0.3) : (40, 50, 70, 1, 2, 3)$, $\sigma^- : \sigma^+ = 1 : 10$, while the third column is the errors when $A^- : A^+ = (20, 30, 20, -3, -1, -2) : (2, 3, 2, -0.3, -0.1, -0.2)$, $\sigma^- : \sigma^+ = 10 : 1$. In Table 4.9, the second column lists the errors of the computed solutions when $A^- : A^+ = (4, 6, 5, 1, 0.5, 0.1) : (4000, 6000, 5000, 1000, 500, 900)$, $\sigma^- : \sigma^+ = 1 : 5000$, while the third column shows the errors when $A^- : A^+ = (1, 2, 3, 0.1, 0.2, 0.3) : (4 \times 10^6, 5 \times 10^6, 6 \times 10^6, 1 \times 10^5, 2 \times 10^5, 3 \times 10^5)$, $\sigma^- : \sigma^+ = 1 : 3 \times 10^6$.

From these two tables and the corresponding linear regression results, we can see a clear second order convergence for both small jumps and large jumps in the anisotropic coefficients.

The linear regression results corresponding to Table 4.8 in Fig. 4.8 provided the convergence order and error constants below:

$$
\| U^h - u \|_\infty \approx 22.3186 \, h^{2.0561}, \quad \| U^h - u \|_\infty \approx 19.4626 \, h^{2.1166}.
$$

The linear regression results corresponding to Table 4.9 in Fig. 4.9 provided the convergence order and error constants below:

$$
\| U^h - u \|_\infty \approx 27.7702 \, h^{2.0396}, \quad \| U^h - u \|_\infty \approx 21.0770 \, h^{2.0366}.
$$

Example 4.6. As suggested by one of referees, we consider an example with large jump ratios in which the anisotropic coefficient $\mathbf{A} = \text{diag}\left(10^6, 1, 10^{-6}\right)$. As we know that efficient numerical methods work well for well-conditioned problems, but may not work well for ill-conditioned problems. When $\mathbf{A} = \text{diag}\left(10^6, 1, 10^{-6}\right)$, the condition number is 10^{12} which is an ill-conditioned problem. A direct application of our method leads to inaccurate computed
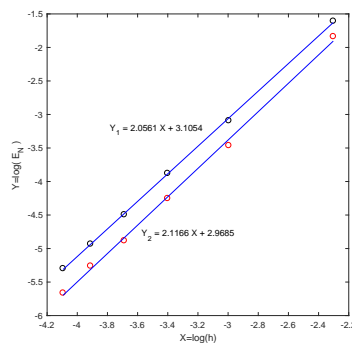

Fig. 4.8. Linear regression of Table 4.8. The average convergence orders are 2.0561 and 2.1166, respectively.

Table 4.9: A grid refinement analysis for Example 4.5 with large jumps in the coefficients.

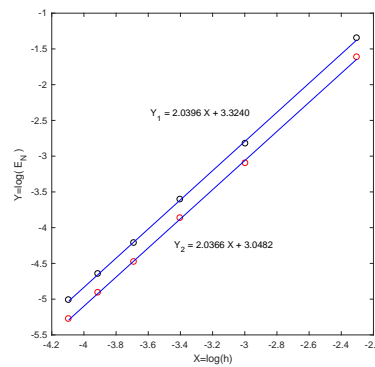| N	$\max\limits_{i,j}\left\{\dfrac{|A_{ij}^+|}{|A_{ij}^-|}\right\} = 9000$	$\max\limits_{i,j}\left\{\dfrac{|A_{ij}^+|}{|A_{ij}^-|}\right\} = 10^6$
	$\|E_N\|_\infty$	$\|E_N\|_\infty$
20	2.5945E-01	1.9877E-01
40	5.9344E-02	4.5099E-02
60	2.7154E-02	2.0940E-02
80	1.4782E-02	1.1342E-02
100	9.5902E-03	7.3745E-03
120	6.6548E-03	5.1060E-03

Fig. 4.9. Linear regression of Table 4.9. The average convergence orders are 2.0396 and 2.0366, respectively.

solution. We have proposed a preconditioning strategy for such problems. For example, if the anisotropic coefficient is given as

$$A^- = \begin{pmatrix} 10^6 & 10^2 & 10^{-3} \\ 10^2 & 1 & 10^{-6} \\ 10^{-3} & 10^{-6} & 10^{-6} \end{pmatrix}, \quad A^+ = \beta A^-,$$

we use a scaling strategy as below

$$\mathbf{y} = D_\Gamma \mathbf{x}, \quad D_\Gamma = \begin{pmatrix} 10^{-3} & 0 & 0 \\ 0 & 1 & 0 \\ 0 & 0 & 10^3 \end{pmatrix}, \quad \mathbf{x} = (x, y, z)^T, \quad \mathbf{y} = (\bar{x}, \bar{y}, \bar{z})^T.$$

Then we use our new method for the following transformed problem

$$-\nabla \cdot \left(\bar{\mathbf{A}} \nabla \bar{u}(\mathbf{y}) \right) = \bar{f}(\mathbf{y}), \tag{4.7}$$

when $\sigma = 0$. The new anisotropic coefficient is

$$\bar{\mathbf{A}}^- = \begin{pmatrix} 1 & 10^{-1} & 10^{-3} \\ 10^{-1} & 1 & 10^{-3} \\ 10^{-3} & 10^{-3} & 1 \end{pmatrix}, \quad \bar{\mathbf{A}}^+ = \beta \bar{\mathbf{A}}^-.$$

The analytic solution and the interface are the same as in Example 4.5.

Table 4.10: A grid refinement analysis for Example 4.6 with $\beta = 10.0$ and $\beta = 1000$.

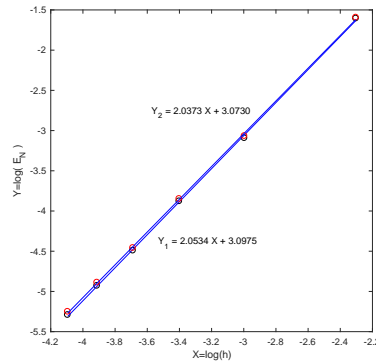| N	$\beta = 10$ $\|E_N\|_\infty$	$\beta = 1000$ $\|E_N\|_\infty$
20	2.0061E-01	2.0296E-01
40	4.5340E-02	4.6526E-02
60	2.0675E-02	2.1291E-02
80	1.1196E-02	1.1571E-02
100	7.2277E-03	7.5267E-03
120	5.0289E-03	5.2366E-03

Fig. 4.10. Linear regression of Table 4.10. The average convergence orders are 2.0534 and 2.0373, respectively.

After the preconditioning, our method worked well for the problem. Note that, the domain will also be changed after the scaling. However, a 3D rectangular domain will still be a 3D rectangular domain and our method can still apply maybe with different mesh size h_x, h_y, and h_z. For convenience, we still use the cubic in the scaled system in our numerical test. In Table 4.10, we show the grid refinement results and linear regression analysis to get the convergence order when $\beta = 10$ and $\beta = 1000$. We can see a second order convergence for both modest jump and large jump in anisotropic coefficients.

The linear regression results corresponding to Table 4.10 in Fig. 4.10 provided the convergence order and error constants below:

$$\| U^h - u \|_\infty \approx 22.1432\, h^{2.0534}, \quad \| U^h - u \|_\infty \approx 21.6056\, h^{2.0373}.$$

Example 4.7. Next, we show a comparison example with the Petrov-Galerkin immersed finite element method in [3], in which

$$A^- = \begin{pmatrix} \cos(x+y)^2 + 3 & z & 0.2\sin(z-x) \\ z & z^2 + 5 & y \\ 0.2\sin(z-x) & y & \sin(z)^2 + 2 \end{pmatrix}, \tag{4.8}$$

$$A^+ = \begin{pmatrix} 4x^2 + 6 & \sin(x+y) & xy \\ \sin(x+y) & 2z^2 + 3 & 0.5\sin(x) \\ xy & 0.5\sin(x) & \cos(xy+z)^2 + 5 \end{pmatrix}, \tag{4.9}$$

Table 4.11: A grid refinement analysis of the proposed method and the method developed in [3] for Example 4.7.

N	FE-FD Method		Method in [3]	
	$\|E\|_\infty$	Order	$\|E\|_\infty$	Order
6	0.02525		0.01579	
12	0.00696	1.86	0.00512	1.62
24	0.00167	2.06	0.00140	1.87
48	0.00048	1.80	0.00035	2.00
Average		1.90		1.83

with $\sigma = 0$, and the analytic solution

$$u(x,y,z) = \begin{cases} -\cos(x) + 3y + z^3 & \text{if } (x,y,z) \in \Omega^-, \\ 5 - \sin(x^3) + 3y^2 + z & \text{if } (x,y,z) \in \Omega^+. \end{cases} \tag{4.10}$$

The interface is a sphere, the zero level set of $\varphi(x,y,z) = 0.25 - x^2 - y^2 - z^2$.

In Table 4.11, we show grid refinement results obtained by our new method and the method developed in [3]. The grid refinement results indicate that the two methods have comparable magnitude of errors and order of convergence. But the convergence of the method in [3] has not been proved theoretically yet except for some simple scalar cases such as for one-dimensional (1D) problems or two-dimensional (2D) problems with line interfaces that are parallel to coordinate axes.

5. Conclusions

In this paper, we have developed a FE-FD method for solving 3D anisotropic elliptic interface problems. The new FE-FD method is a Cartesian mesh method. For regular grid points, we apply a fifteen-point stencil scheme, which is derived from the linear finite element method based on a uniform tetrahedralization, and corresponding discrete matrix of the linear system of equations is symmetric semi-positive definite. For irregular grid points, we have derived new interface relations and constructed a maximum principle preserving finite difference scheme using these new jump relations and a quadratic constraint optimization. The resulting coefficient matrix of linear system of equations is an M-matrix. The mew method is tested with non-homogeneous/homogeneous jump conditions and singular source terms. Both theoretical analysis and numerical results show that the computed solution have second order convergence in the infinity norm.

A. Coefficients Relations Use in Theorem 3.1

We list the definition of the unspecified coefficients in Theorem 3.1 below.

$$d_1 = \chi_{\eta\eta} a_{12}^+ + \chi_{\eta\tau} a_{13}^+, \quad d_2 = \chi_{\eta\eta} a_{22}^+ + \chi_{\eta\tau} a_{23}^+, \quad d_3 = \chi_{\eta\eta} a_{23}^+ + \chi_{\eta\tau} a_{33}^+,$$

$$d_4 = \chi_{\eta\tau}a_{12}^+ + \chi_{\tau\tau}a_{13}^+, \quad d_5 = \chi_{\eta\tau}a_{22}^+ + \chi_{\tau\tau}a_{23}^+, \quad d_6 = \chi_{\eta\tau}a_{23}^+ + \chi_{\tau\tau}a_{33}^+,$$

$$S_{m0} = \frac{\chi_{\eta\eta}a_{22}^+ + \chi_{\tau\tau}a_{33}^+ + 2\chi_{\eta\tau}a_{23}^+}{a_{11}^+},$$

$$S_{m1} = \frac{a_{11}^+[d_1] - \left(d_1^+ + \chi_{\eta\eta}a_{12}^+ + \chi_{\eta\tau}a_{13}^+\right)[a_{11}^+]}{(a_{11}^+)^2},$$

$$S_{m2} = \frac{a_{11}^+[d_4] - \left(d_4^+ + \chi_{\eta\tau}a_{12}^+ + \chi_{\tau\tau}a_{13}^+\right)[a_{11}^+]}{(a_{11}^+)^2},$$

$$S_{m3} = \frac{a_{11}^+[d_2] - \left(d_1^+ + \chi_{\eta\eta}a_{12}^+ + \chi_{\eta\tau}a_{13}^+\right)[a_{12}^+]}{(a_{11}^+)^2},$$

$$S_{m4} = \frac{a_{11}^+[d_5] - \left(d_4^+ + \chi_{\eta\tau}a_{12}^+ + \chi_{\tau\tau}a_{13}^+\right)[a_{12}^+]}{(a_{11}^+)^2},$$

$$S_{m5} = \frac{a_{11}^+[d_3] - \left(d_1^+ + \chi_{\eta\eta}a_{12}^+ + \chi_{\eta\tau}a_{13}^+\right)[a_{13}^+]}{(a_{11}^+)^2},$$

$$S_{m6} = \frac{a_{11}^+[d_6] - \left(d_4^+ + \chi_{\eta\tau}a_{12}^+ + \chi_{\tau\tau}a_{13}^+\right)[a_{13}^+]}{(a_{11}^+)^2},$$

$$S_{m7} = \frac{\chi_{\eta\eta}b_{12} + \chi_{\tau\tau}b_{14} + \chi_{\eta\tau}b_{20}}{a_{11}^+},$$

$$S_{n1} = \frac{a_{11}^+d_2^+ - \left(d_1^+ + \chi_{\eta\eta}a_{12}^+ + \chi_{\eta\tau}a_{13}^+\right)a_{12}^+}{(a_{11}^+)^2},$$

$$S_{n2} = \frac{a_{11}^+d_5^+ - \left(d_4^+ + \chi_{\eta\tau}a_{12}^+ + \chi_{\tau\tau}a_{13}^+\right)a_{12}^+}{(a_{11}^+)^2},$$

$$S_{n3} = \frac{a_{11}^+d_3^+ - \left(d_1^+ + \chi_{\eta\eta}a_{12}^+ + \chi_{\eta\tau}a_{13}^+\right)a_{13}^+}{(a_{11}^+)^2},$$

$$S_{n4} = \frac{a_{11}^+d_6^+ - \left(d_4^+ + \chi_{\eta\tau}a_{12}^+ + \chi_{\tau\tau}a_{13}^+\right)a_{13}^+}{(a_{11}^+)^2},$$

$$S_{n5} = \frac{d_1^+ + \chi_{\eta\eta}a_{12}^+ + \chi_{\eta\tau}a_{13}^+}{(a_{11}^+)^2}, \qquad S_{n6} = \frac{d_4^+ + \chi_{\eta\tau}a_{12}^+ + \chi_{\tau\tau}a_{13}^+}{(a_{11}^+)^2},$$

$$C_{1,1} = -\frac{1}{a_{11}^+}\left(S_{m0}[a_{11}] + 2a_{12}^+S_{m1} + 2a_{13}^+S_{m2}\right),$$

$$C_{1,2} = -\frac{1}{a_{11}^+}\left(S_{m0}[a_{12}] + 2a_{12}^+S_{m3} + 2a_{13}^+S_{m4}\right),$$

$$C_{1,3} = -\frac{1}{a_{11}^+}\left(S_{m0}[a_{13}] + 2a_{12}^+S_{m5} + 2a_{13}^+S_{m6}\right),$$

$$C_{1,4} = -\frac{1}{a_{11}^+}\left(S_{m0}a_{12}^+ + 2a_{12}^+S_{n1} + 2a_{13}^+S_{n2}\right),$$

$$C_{1,5} = -\frac{1}{a_{11}^+}\left(S_{m0}a_{13}^+ + 2a_{12}^+S_{n3} + 2a_{13}^+S_{n4}\right),$$

$$C_{1,6} = \frac{1}{a_{11}^+}\left(S_{m0} - 2a_{12}^+S_{n5} - 2a_{13}^+S_{n6}\right).$$

B. Jump Relations for a Variable Coefficients $\mathbf{A}(x, y, z)$

If the coefficient matrix $\mathbf{A}(x, y, z)$ and $\sigma(x, y, y)$ are piecewise variable, the last three identities in Theorem 3.1 need to be changed. For the eighth and ninth interface relations, we need to redefine $d_j, j = 1, 2, 3, 4, 5, 6$ as follows,

$$d_1 = \chi_{\eta\eta} a_{12}^+ + \chi_{\eta\tau} a_{13}^+ - \frac{\partial a_{11}^+}{\partial \eta}, \qquad d_2 = \chi_{\eta\eta} a_{22}^+ + \chi_{\eta\tau} a_{23}^+ - \frac{\partial a_{12}^+}{\partial \eta},$$

$$d_3 = \chi_{\eta\eta} a_{23}^+ + \chi_{\eta\tau} a_{33}^+ - \frac{\partial a_{13}^+}{\partial \eta}, \qquad d_4 = \chi_{\eta\tau} a_{12}^+ + \chi_{\tau\tau} a_{13}^+ - \frac{\partial a_{11}^+}{\partial \tau},$$

$$d_5 = \chi_{\eta\tau} a_{22}^+ + \chi_{\tau\tau} a_{23}^+ - \frac{\partial a_{12}^+}{\partial \tau}, \qquad d_6 = \chi_{\eta\tau} a_{23}^+ + \chi_{\tau\tau} a_{33}^+ - \frac{\partial a_{13}^+}{\partial \tau}.$$

In the local coordinates, the PDE becomes

$$-(a_{11} u_{\xi\xi} + a_{22} u_{\eta\eta} + a_{33} u_{\tau\tau} + 2a_{12} u_{\xi\eta} + 2a_{13} u_{\xi\tau} + 2a_{23} u_{\eta\tau} + c_1 u_\xi + c_2 u_\eta + c_3 u_\tau) + \sigma u = f,$$

where

$$c_1 = \frac{\partial a_{11}}{\partial \xi} + \frac{\partial a_{12}}{\partial \eta} + \frac{\partial a_{13}}{\partial \tau}, \quad c_2 = \frac{\partial a_{12}}{\partial \xi} + \frac{\partial a_{22}}{\partial \eta} + \frac{\partial a_{23}}{\partial \tau}, \quad c_3 = \frac{\partial a_{13}}{\partial \xi} + \frac{\partial a_{23}}{\partial \eta} + \frac{\partial a_{33}}{\partial \tau}.$$

This leads to the last relation followed by some terms about $c_j^\pm, j = 1, 2, 3$ as below

$$u_{\xi\xi} = S + \frac{a_{11}^+ c_1^- - a_{11}^- c_1^+}{(a_{11}^+)^2} u_\xi + \frac{c_1^+ [a_{12}] - a_{11}^+ [c_2]}{(a_{11}^+)^2} u_\eta + \frac{c_1^+ [a_{13}] - a_{11}^+ [c_3]}{(a_{11}^+)^2} u_\tau$$
$$+ \frac{a_{12}^+ c_1^+ - a_{11}^+ c_2^+}{(a_{11}^+)^2} w_\eta + \frac{a_{13}^+ c_1^+ - a_{11}^+ c_3^+}{(a_{11}^+)^2} w_\tau - \frac{c_1^+}{(a_{11}^+)^2} Q,$$

where S is the term of the right hand side defined in the last relation in Theorem 3.1.

References

[1] L.C. Evans, *Partial Differential Equations*, 1st ed., American Mathematical Society, Berkeley, 1998.

[2] N. An and H. Chen, A partially penalty immersed interface finite element method for anisotropic elliptic interface problems. *Numerical Methods for Partial Differential Equations*, **30** (2014), 1984–2028.

[3] S. Hou, P. Song, L. Wang, and H.K. Zhao, A weak formulation for solving elliptic interface problems without body fitted grid. *Journal of Computational Physics*, **249** (2013), 80–95.

[4] S. Hou, W. Wang and L. Wang, Numerical method for solving matrix coefficient elliptic equation with sharp-edged interfaces. *Journal of Computational Physics*, **229** (2010), 7162–7179.

[5] L. Wang, S. Hou and L. Shi, A numerical method for solving three-dimensional elliptic interface problems with triple junction points. *Advances in Computational Mathematics*, **44** (2018), 175–193.

[6] C. Lu, Z. Yang, J. Bai, Y. Cao and X. He, Three-dimensional immersed finite-element method for anisotropic magnetostatic/electrostatic interface problems with nonhomogeneous flux jump. *International Journal for Numerical Methods in Engineering*, **121** (2020), 2107–2127.

[7] M. Dumett and J. Keener, An immersed interface method for solving anisotropic elliptic boundary value problems in three dimensions. *SIAM Journal on Scientific Computing*. **25** (2003), 348–367.

[8] B. Dong, X. Feng and Z. Li, A FE-FD method for anisotropic elliptic interface problems. *SIAM Journal on Scientific Computing*. **42** (2020), B1041–B1066.

[9] Y. Gong, B. Li and Z. Li, Immersed-interfacefinite-element methods for elliptic interface problems with non-homogeneous jump conditions. *SIAM Journal on Numerical Analysis*, **46** (2008), 472–495.

[10] D. Braess, *Finite elements: Theory, fast solvers, and applications in solid mechanics*, 3rd ed., Cambridge University Press, Cambridge, 2007.

[11] S.C. Brenner and L.R. Scott, *The mathematical theory of finite element methods*, 3rd ed., Springer, New York, 2002.

[12] J.H. Bramble and V. Thomée, Interior maximum norm estimates for some simple finite element methods. *ESAIM: Mathematical Modelling and Numerical Analysis*, **8** (1974), 5–18.

[13] E. Dari, R.G. Duran and C. Padra, Maximum norm error estimators for three-dimensional elliptic problems. *SIAM Journal on Numerical Analysis*, **37** (2000), 683–700.

[14] R. Scott, Optimal L^∞ estimates for the finite element method on irregular meshes. *Mathematics of Computation*, **30**:136 (1976), 681–697.

[15] S. Deng, K. Ito and Z. Li, Three dimensional elliptic solvers for interface problems and applications. *Journal of Computational Physics*, **184** (2003), 215–243.

[16] Z. Li, and K. Ito, Maximum principle preserving schemes for interface problems with discontinuous coefficients. *SIAM Journal on Scientific Computing*, **23** (2001), 1225–1242.

[17] K. Schittkowski, *QL-quadratic Programming*, Version 1.5, 1991, http://www.uni-bayreuth .de/departments/math/ kschittkowski/ql.htm.

[18] I. Babuška, The finite element method for elliptic equations with discontinuous coefficients. *Computing*, **5**:3 (1970), 207–213.

[19] K.W. Morton and D.F. Mayers, *Numerical solution of partial differential equations*, 1st ed., Cambridge University Press, Cambridge, 1995.